5. Conclusions

Here, we developed a portable container to constantly keep the inner temperature without any batteries or energy source. Cells cultured on temperature-responsive culture dishes were successfully transported with the container, and transplantable cell sheets were harvested after 8 h transportation by car. Such a device would promote regenerative medicine in clinical settings.

Acknowledgements

We would like to thank Dr Masato Kanzaki (Tokyo Women's Medical University) for technical criticism. We are also grateful for valuable comments from Mr Kazutoshi Kan and Mr Shio Miyamoto (Hitachi Ltd) as well as Mr Takashi Matsuoka (Hitachi Transport System Ltd). This work was supported in part by the Centre of Excellence (COE) Programme for the Twenty-first Century, and the High-Tech Research Centre Programme from the Ministry of Education, Culture, Sports, Science and Technology (MEXT), Japan.

References

Kushida A, Yamato M, Isoi Y, *et al.* 2005; A noninvasive transfer system for polarized renal tubule epithelial cell sheets using temperature-responsive culture dishes. *Eur Cell Mater* **10**: 23–30.

Kushida A, Yamato M, Kikuchi A, *et al.* 2001; Two-dimensional manipulation of differentiated Madin–Darby canine kidney (MDCK) cell sheets: the noninvasive harvest from temperature-responsive culture dishes and transfer to other surfaces. *J Biomed Mater Res* **54**: 37–46.

Kushida A, Yamato M, Konno C, *et al.* 1999; Decrease in culture temperature releases monolayer endothelial cell sheets together with deposited fibronectin matrix from temperature-responsive culture surfaces. *J Biomed Mater Res* **45**: 355–362.

Murakami D, Yamato M, Nishida K, *et al.* 2006; The effect of micropores in the surface of temperature-responsive culture inserts on the fabrication of transplantable canine oral mucosal epithelial cell sheets. *Biomaterials* **27**: 5518–5523.

Nishida K, Yamato M, Hayashida Y, *et al.* 2004; Corneal reconstruction with tissue-engineered cell sheets composed of autologous oral mucosal epithelium. *N Engl J Med* **351**: 1187–1196.

Shimizu T, Yamato M, Isoi Y, *et al.* 2002; Fabrication of pulsatile cardiac tissue grafts using a novel 3-dimensional cell sheet manipulation technique and temperature-responsive cell culture surfaces. *Circ Res* **90**: e40.

Yamada N, Okano T, Sakai H, *et al.* 1990; Thermo-responsive polymeric surfaces; control of attachment and detachment of cultured cells. *Macromol Chem Rapid Commun* **11**: 571–576.

Yamato M, Utsumi M, Kushida A, *et al.* 2001; Thermo-responsive culture dishes allow the intact harvest of multilayered keratinocyte sheets without dispase by reducing temperature. *Tissue Eng* **7**: 473–480.

Yang J, Yamato M, Nishida K, *et al.* 2006; Cell delivery in regenerative medicine: the cell sheet engineering approach. *J Control Release* **116**: 193–203.

Biomaterials 29 (2008) 2565–2572

Contents lists available at ScienceDirect

Biomaterials

journal homepage: www.elsevier.com/locate/biomaterials

A thermoresponsive, microtextured substrate for cell sheet engineering with defined structural organization

Brett C. Isenberg [a], Yukiko Tsuda [b], Corin Williams [a], Tatsuya Shimizu [b], Masayuki Yamato [b], Teruo Okano [b], Joyce Y. Wong [a,*]

[a] Department of Biomedical Engineering, Boston University, 44 Cummington Street, Boston, MA 02215, USA
[b] Institute of Advanced Biomedical Engineering and Science, Tokyo Women's Medical University, 8-1 Kawadacho, Shinjuku, Tokyo 162-8666, Japan

ARTICLE INFO

Article history:
Received 3 January 2008
Accepted 28 February 2008
Available online 30 March 2008

Keywords:
Thermoresponsive surfaces
Surface topography
Embossing
Cell sheet
Tissue engineering
Smooth muscle cell

ABSTRACT

The proper function of many tissues depends critically on the structural organization of the cells and matrix of which they are comprised. Therefore, in order to engineer functional tissue equivalents that closely mimic the unique properties of native tissues it is necessary to develop strategies for reproducing the complex, highly organized structure of these tissues. To this end, we sought to develop a simple method for generating cell sheets that have defined ECM/cell organization using microtextured, thermoresponsive polystyrene substrates to guide cell organization and tissue growth. The patterns consisted of large arrays of alternating grooves and ridges (50 μm wide, 5 μm deep). Vascular smooth muscle cells cultured on these substrates produced intact sheets consisting of cells that exhibited strong alignment in the direction of the micropattern. These sheets could be readily transferred from patterned substrates to non-patterned substrates without the loss of tissue organization. Ultimately, such sheets will be layered to form larger tissues with defined ECM/cell organization that spans multiple length scales.

1. Introduction

The structural organization of cells and extracellular matrix (ECM) in native tissues is crucial for proper function, particularly in load-bearing and muscular tissues [1]. Therefore, as the field of tissue engineering matures and begins to move towards creating larger, more complicated tissues and organs, the need arises to develop strategies for growing tissues with precise structural features that can be controlled over multiple length scales. Currently, many popular approaches to tissue construction employ isotropic scaffolds or substrates that do not possess any specific organizational cues to guide tissue development, resulting in tissues that rarely possess the structural properties of the native tissues that they are designed to replace. For example, this is the case for arterial tissue, where the development of a functional tissue engineered artery that possesses the unique, anisotropic mechanical properties of the native vessel remains elusive [2–4]. This is due, in part, to the difficulty in adequately mimicking the structural organization of the artery wall, which derives its properties from its complex organization of matrix proteins and cells [5–7]. The medial layer of the artery wall is believed to be the principal load-bearing layer and is composed of alternating layers of smooth muscle cells (SMCs) embedded in collagen and elastin lamellae. The collagen and SMCs are arranged in a helical pattern around the circumference of the vessel, with the direction of the pitch alternating between successive layers [8]. This helical arrangement not only provides enhanced circumferential load-bearing properties to the tissue, but also imparts torsional stability. Furthermore, this arrangement of the SMCs allows for more efficient control of vessel tone (which in turn dictates blood pressure and shear stress) as this configuration leads to SMC contraction that primarily results in a reduction of the vessel lumen diameter rather than its length. Attempts to specifically engineer such organization into tissue engineered arteries have met with differing degrees of success. While biopolymer-based tissues have been shown to possess the proper alignment of matrix components [9–11] and exhibit mechanical anisotropy [12], their overall mechanical properties are not sufficient for implantation [13]. On the other hand, tissue engineered grafts made solely from cell-secreted ECM, using a "self-assembly" or cell sheet-based approach, could support high burst pressures and have shown success in vivo, yet lacked the desired organization [14]. However, further refinement of this approach using static mechanical load to align matured cell sheets has resulted in tissues with the desired cell/matrix organization and mechanical anisotropy [15]. These results are extremely encouraging, however, this method requires increasing

* Corresponding author. Tel.: +1 617 353 2374; fax: +1 617 353 6766.
E-mail address: jywong@bu.edu (J.Y. Wong).

0142-9612/$ – see front matter © 2008 Elsevier Ltd. All rights reserved.
doi:10.1016/j.biomaterials.2008.02.023

the already lengthy incubation time in order to generate such organization.

Cell sheet engineering has arisen recently as an attractive approach to tissue engineering. In this approach, confluent cell cultures are harvested from a variety of substrates as intact, tissue-like sheets consisting of the cells and their associated extracellular matrix (ECM) [16,17]. These sheets can then be used individually or layered/rolled to create tissues of larger size or with defined laminar organization. In particular, cell sheet engineering using thermoresponsive cell culture substrates has enabled this approach to be extended to a wide variety of tissue types and therapies [17]. Tissue culture dishes treated with a thin layer of the thermoresponsive polymer poly(*N*-isopropylacrylamide) (PIPAAm) can support cell adhesion and growth at 37 °C (where the PIPAAm is hydrophobic) [18], while lowering the temperature below its lower critical solution temperature (32 °C) causes the polymer to become hydrophilic and swell [19]. This swelling induces the cells and any associated ECM to lift off the surface of the culture dish while maintaining cell–cell and cell–ECM connections [20–24], which are crucial for proper tissue function. This is in contrast to typical methods of cell adhesion disruption that usually include treatment with digestive enzymes, such as trypsin, that destroy these important connections. While this technology has proven to be a highly effective means of engineering tissues, the resulting cell sheets lack any sort of structural organization due to a lack of organizational cues from the substrates. Methods have been developed to prepare substrates to control the spatial distribution of cells [25,26], but these approaches require multiple complicated steps and were designed with spatially segregating multiple cell types as opposed to defining the structural organization of the cells and matrix themselves.

Micropatterning has been widely used as a method of controlling cell morphology, spatial arrangement, and function [27,28] by imparting various types of cell-scale guidance cues by controlling regions of adhesion [25,29–31], topology [32–37], and "direct writing" of scaffolds and cells [38–40]. A common method used in many of these approaches involves a set of techniques known as soft lithography [41]. Soft lithography uses a stamp or mold prepared by casting an elastomer, typically polydimethylsiloxane (PDMS), against a master containing a patterned relief structure prepared via traditional photolithography techniques. These materials can then serve as stamps that can be used to deposit molecules in precise patterns via microcontact printing in order to spatially control cell adhesion [29,31], as well as being used as topological cues themselves, mimicking the 3-dimensional nano- and microstructure of the native ECM [34]. A particularly attractive use for these molds is for hot embossing of thermoplastic polymers (e.g., polystyrene (PS)) in order to create substrates with topological features on the micron- and submicron-scale [32,37,42]. By pressing a micropatterned PDMS mold against a thin sheet of PS and heating it above the glass transition temperature of PS, it is possible to accurately and reproducibly transfer a micropattern from a PDMS mold to a PS substrate [32]. This technique provides a simple, single-step method of micropatterning substrates while maintaining chemical uniformity at the surface, which is not possible with microcontact printing, making them ideal for grafting with PIPAAm using published protocols [18].

By combining the techniques of hot embossing and PIPAAm grafting, we have been able to generate thermoresponsive, microtextured substrates that support cell adhesion and growth. Here, we describe a simple technique for creating such substrates and examine the morphological properties of the resulting cell sheets. SMCs grown on these substrates conformed to the topology of the substrates by orienting in the direction of microtextured grooves and quickly grew to confluence over the entire surface of the substrates. The resulting cell sheets could be easily detached from the substrates by simply lowering the culture temperature and transferred to non-patterned substrates without loss of cell or ECM organization.

2. Materials and methods

2.1. Microtexturing

Microtextured polystyrene substrates were prepared by hot embossing thin polystyrene films with microtextured polydimethylsiloxane (PDMS) molds containing an array of parallel grooves (50 μm wide, spaced 50 μm apart, 5 μm deep). The PDMS molds were generated using conventional photolithography and soft lithography techniques as previously described [34]. Briefly, patterned silicon wafers were made by applying a layer of SU-8 3005 photoresist (MicroChem Corp., Newton, MA, USA) onto 4-inch silicon wafers using a spincoater (Active Co., Ltd., Saitama City, Japan). The wafers were exposed to UV light through a patterned photomask using a BA100 mask aligner (Nanometric Technology, Inc., Tokyo, Japan) and developed using ethyl lactate. The patterned wafers were then silanized using a solution of 2% dimethyloctadecylchlorosilane (Shin Etsu Chemical Co., Ltd., Tokyo, Japan) in toluene before curing PDMS (Silpot 184, Dow Corning, Tokyo, Japan) against the patterned wafers. Removal of the PDMS from the wafers (facilitated by the silanization treatment) yielded microtextured PDMS master molds. It should be noted that the printing process yielded photomasks with lines slightly wider than the expected 50 μm, resulting in ridges on the wafers that were slightly wider (51.4 ± 1.4 μm) than the grooves (49.0 ± 0.7 μm).

Hot embossing of the polystyrene (PS) was accomplished by pressing the microtextured PDMS master molds against a 250-μm thick PS sheet (a kind gift from Mitsubishi Chemical Co., Tokyo, Japan) using a custom-built device (Fig. 1) in an oven for 5 min at 200 °C. Non-microtextured control substrates were generated by using a non-microtextured PDMS mold instead of a microtextured PDMS mold. Upon removal from the oven, the device was allowed to cool for at least 5 min before removing the PS sheet from the device. The sheets were washed several times in ethanol and examined using a scanning electron microscope to verify that the pattern was properly transferred from the PDMS to the PS. The PDMS molds could be reused more than 50 times without loss or damage to the micropattern.

2.2. Polymer grafting

Microtextured and non-microtextured PS substrates were grafted with PIPAAm as described previously for TCPS dishes [43]. Briefly, IPAAm monomer (a kind gift from Kohjin Co. Ltd., Tokyo, Japan) was first purified by recrystallization from *n*-hexane. A thin layer of IPAAm solution (dissolved in 2-propanol) was spread over the upper surface of PS substrates (i.e., textured surface), which were subsequently exposed to electron beam irradiation using an Area Beam Electron-Processing System (Nissin-High Voltage Co. Ltd., Kyoto, Japan), resulting in polymerization and covalent grafting onto the PS sheets. Grafted substrates were washed overnight in deionized water and subsequently dried at 45 °C. Substrates grafted with solutions containing 40%, 45%, 50%, and 55% IPAAm were investigated in this study.

2.3. Scanning electron microscopy of substrate surfaces

PDMS, non-grafted microtextured PS and PIPAAm-grafted microtextured PS substrates were examined with a scanning electron microscope (VE-9800, KEYENCE Co., Osaka, Japan). Samples did not require surface treatment to enhance visualization.

2.4. Cell seeding

Grafted and un-grafted microtextured PS substrates as well as grafted and un-grafted non-microtextured PS substrates were sterilized by soaking in 70% ethanol for 1 h, transferring them to sterile culture dishes where they were allowed to dry completely, and finally exposing them to UV light in a clean bench for 30 min. To promote cell attachment, substrates were incubated overnight in fetal bovine serum at 37 °C. Adult human aortic smooth muscle cells (AoSMCs) (Lonza, Basel, Switzerland) were seeded onto substrates at a concentration of 40,000 cells/cm^2. Seeded substrates were cultured in SmGM-2 medium (Lonza) for up to two weeks post-seeding. AoSMCs between passages 7 and 10 were used in this study.

2.5. Cell orientation and elongation

To investigate the orientation of the cells on both microtextured and non-microtextured substrates, cell nuclei were stained by incubating the cultures in standard culture medium containing Hoechst 33342 (Molecular Probes, Carlsbad, CA, USA) at a dilution of 1:1000 for 30 min. The cultures were then washed three times with PBS and immediately imaged under epifluorescence using an Eclipse TE2000-U microscope (Nikon, Tokyo, Japan) and processed with Axio Vision v4.2 (Carl Zeiss, Oberkochen, Germany). For each substrate, five images were taken at random locations. Cell orientation was assessed by measuring the angle between the long axis of the nucleus [44] and the direction of the grooves using ImageJ

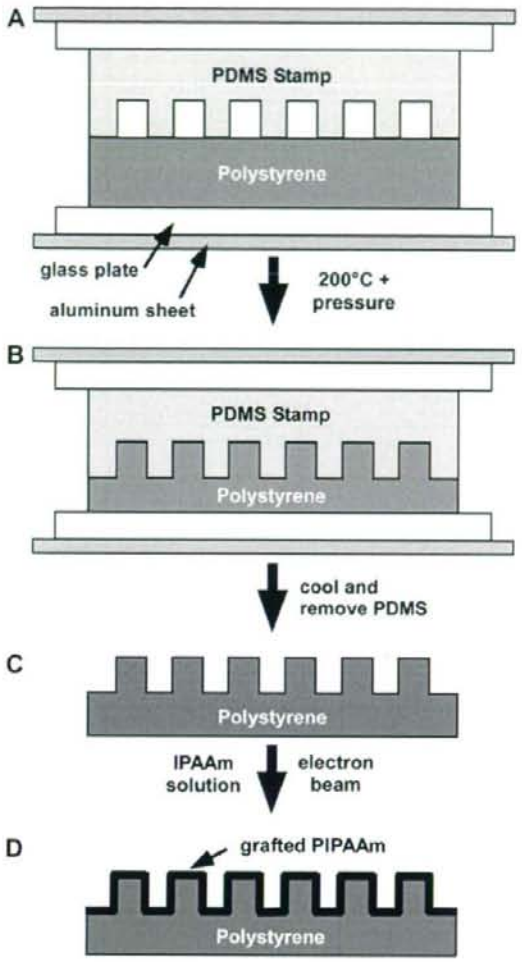

Fig. 1. Polystyrene substrate microtexturing and PIPAAm grafting. Hot embossing of the PS sheets was accomplished by pressing the microtextured PDMS master molds against a polystyrene sheet between aluminum and glass plates using a custom-built device (A). This device was placed in an oven for 5 min at 200 °C (B) and subsequently cooled for 5 min before removing the PS sheet from the device (C). PS substrates were grafted with PIPAAm by first applying a thin layer of IPAAm dissolved in isopropanol to the surface of the substrate and then exposing them to electron beam irradiation (D). Grafted substrates were washed overnight in deionized water and subsequently dried at 45 °C. Pattern dimensions are exaggerated for illustrative purposes.

v1.38 (NIH, Bethesda, MD, USA). For non-microtextured substrates, this angle was arbitrarily chosen for each image.

Cytoskeletal organization was assessed by staining F-actin fibrils in the cell sheets with phalloidin. Briefly, samples were fixed with pre-warmed 4% paraformaldehyde for 15 min and then rinsed three times with phosphate buffered saline (PBS). Next, cells were permeabilized with 0.5% TritonX-100 (Sigma) for 10 min at room temperature and rinsed three times with PBS. Samples were blocked with 0.1% bovine serum albumin (BSA) solution for 1 h at 37 °C and then incubated with Alexa Fluor 568 Phalloidin (Molecular Probes; 1:200 dilution) for 2 h at 37 °C. Samples were rinsed three times with BSA, covered with fresh PBS, and then imaged.

2.6. Cell sheet detachment and transfer

For confirmation of the thermoresponsive nature of the substrates, the temperature of the cultures was dropped to 20 °C and imaged at 5- and 45-min time points to assess cell detachment. Transfer of cell sheets from one surface to another was performed using the protocol described by Tsuda et al. [26]. Briefly, a custom-built sheet manipulator was coated with a thin layer of gelatin (1.5 mm thick) and then placed over the top of a cell sheet and incubated for 20 min at 20 °C, allowing the cell sheet to detach from the culture dish and adhere to the gelatin. The manipulator was then removed from the culture dish (with the cell sheet attached), transferred to another dish, and incubated for 20 min at 20 °C. Cell culture medium at 37 °C was then added for 15 min in order for the cell sheet to adhere to the new substrate and the gelatin to melt. The medium (containing the gelatin) was aspirated and fresh medium was carefully added to the new culture dishes.

3. Results

3.1. Substrate topology

The double transfer of the micropattern (silicon wafer to PDMS to PS) should result in the micropattern on the PS sheets being the same as the one on the silicon wafers. SEM images of the substrates confirmed that the micropattern was accurately transferred from the wafer to the PDMS molds and from the PDMS to the PS sheets (Fig. 2). The ridges were slightly wider than the grooves for the reasons noted in Section 2. The depth of the grooves was approximately 5 μm.

3.2. Cell sheet detachment

Cell sheets could be easily detached from the PIPAAm-grafted microtextured PS substrates by reducing the temperature of the cultures to 20 °C (Fig. 3). As expected, cell sheets grown on substrates that had not been grafted with PIPAAm did not detach. Substrates grafted with 40% IPAAm did not support cell sheet detachment within 45 min. In fact, these sheets, as well as the sheets on substrates without PIPAAm, did not detach after 24 h at 20 °C (data not shown). Cell sheets grown on substrates made with 45% and 50% IPAAm began to detach within 5 min and could be completely removed within 45 min. Sheets grown on substrates made with 55% IPAAm began to detach within 45 min, but the sheets did not detach as intact sheets. Cells grown on sheets at this concentration occasionally exhibited clumping behavior and did not always achieve confluence (data not shown), indicating that unlike substrates grafted with 40–50% PIPAAm, substrates grafted with 55% PIPAAm did not fully support cell growth and sheet formation.

3.3. Cell orientation in cell sheets pre- and post-transfer

Fig. 4 shows that cells grown on microtextured regions of the substrate oriented and elongated in the direction of the microtextured grooves, while cells on non-patterned regions did not appear to adopt any preferential orientation. This orientation was maintained following transfer of the cell sheets from PIPAAm-grafted microtextured PS substrates to normal, non-textured TCPS dishes using the gelatin manipulator technique (Fig. 5). This result was further confirmed by assessing the cytoskeletal organization (F-actin fibrils) of the cells in the cell sheets before and after sheet transfer (Fig. 6), which showed random organization on non-patterned substrates and highly oriented organization on microtextured substrates both before and after cell sheet transfer to TCPS substrates.

The orientation results were quantified by measuring the angle between the long axis of the nucleus and the direction of the grooves of cells grown on microtextured and non-microtextured substrates, both pre- and post-transfer (Fig. 7). Most cells on microtextured substrates (95.7%) had orientation angles <30° (total cells measured, $n = 837$), while cells on non-microtextured substrates had only 30.2% oriented in this direction with similar amounts oriented between 30–60° (36.5%) and 60–90° (33.3%) ($n = 696$), indicating that these cells were randomly oriented. Following cell

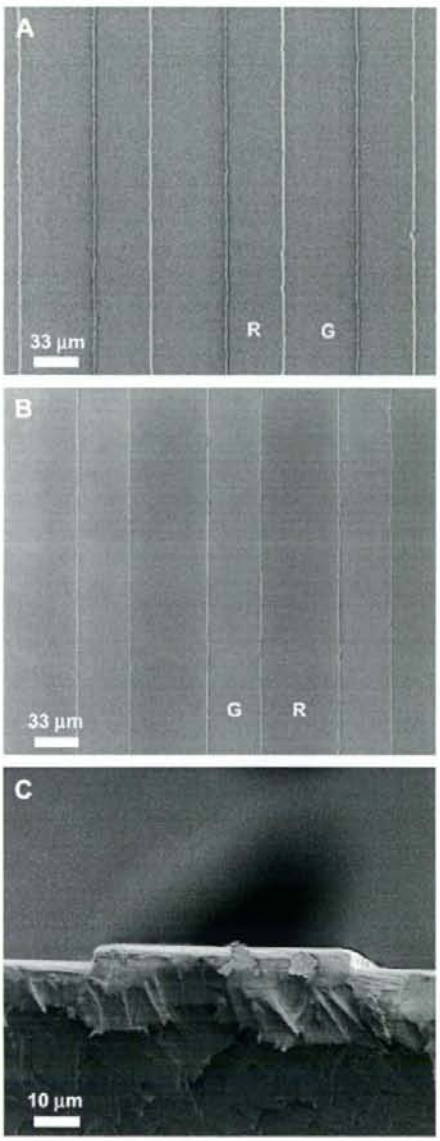

Fig. 2. SEM of microtextured substrates. Scanning electron microscopic images of PS substrates show accurate transfer of the microtexture from the PDMS mold (A) to the PS substrate (B). The ridge and groove regions of the substrates are marked with R and G, respectively. Panel C shows a cross-section of a microtextured PS substrate showing that the microtexture height is approximately 5 μm.

sheet transfer, there was no appreciable difference between the cell orientation angle distribution of the cell sheets before ($n = 837$) and after ($n = 1032$) transfer with a majority of cells having orientation angles $<30°$ (95.7% and 93.5%, respectively), indicating that the microtextured substrate is not required to maintain cell orientation. As expected, the orientation angle distribution of cells grown on non-microtextured substrates was isotropic before ($n = 696$) and after ($n = 957$) sheet transfer.

4. Discussion

Given that the structural organization of tissues is a key factor in governing and maintaining tissue function, particularly in load-bearing and muscular tissues [1], we would like to understand how biomaterials can be used to guide the process of recapitulating native tissue organization. Individual cells are capable of modifying their local microenvironment, but are rarely capable of organizing themselves over length scales required for tissue-level function. Achieving this high level of organization requires a template with the appropriate spatial, biological, and biophysical cues that enable the cells to organize over such length scales. To this end, we have sought to develop a simple technique for engineering tissues with defined organization by combining the well-studied concepts of cell sheet engineering and micropatterning.

Cell sheet engineering using thermoresponsive substrates is an attractive tool for the development of engineered tissues that utilizes simple building blocks (single cell sheets) to construct thick, dense tissues and forgoes the need for implantable scaffolds [17]. However, most sheets produced with this technology possess cells with random orientation and disorganized extracellular matrix. Constructing tissues with structural control at the nano- and micro-scale requires biomaterial substrates that contain chemical and topological features on these length scales. Other attempts at creating cell sheets with complex patterns required complicated, multi-step application of surface coatings and cells [25,26,45] and have been limited to flat substrates. Microtexturing offers the advantage of providing a patterned substrate for cell growth with a contiguous layer of grafted PIPAAm, as opposed to patterned substrates that rely on regions of differing adhesion, allowing the cells to easily and quickly achieve full confluence in a single step. The combination of soft lithography and hot embossing employed in this study provided a simple method for producing materials patterned with feature sizes on the order of tens of microns. The data presented here are based on substrates consisting of parallel grooves 5 μm in depth and 50 μm wide, spaced 50 μm apart. The selection of this set of parameters was somewhat arbitrary as we have been able to achieve similar results with different combinations of groove width and spacing (20–80 μm; data not shown). Significantly deeper grooves have not been investigated; however, since tissues on the order of tens of microns thick are expected from cell sheet techniques, substrates with significantly deeper grooves may have an adverse effect on the resulting cell sheets. The thickness of the tissue growing on the ridges of such a substrate would be significantly thinner than the tissue in the grooves leading to an apparent weakening of the tissue in the direction perpendicular to the grooves. As the tissue will only be as strong as the thinnest region, this could potentially make such sheets more prone to tearing along the thinner ridge regions during handling. Furthermore, deeper grooves would likely lead to an increase in the time required for an intact sheet to form as the cells tend to first settle in the grooves and then grown onto the ridges. For the shallow grooves used here, this process occurs rather quickly (24–48 h), presumably because the 5 μm depth does not provide a significant barrier for the cells to overcome, something which could potentially be an issue for cells grown on deeper grooves. As long as the chosen dimensions of the pattern induce the cells to orient with respect to the pattern, organized cell sheets can be grown; however, it is not clear whether the specific choice of pattern dimensions influences the long-term development of the cell sheet.

The dependence of cell sheet detachment on PIPAAm grafting density is interesting, if not particularly surprising. It is assumed that the cell sheet adhesion is disrupted when grafted PIPAAm layer swells when the culture temperature is dropped below its lower critical solution temperature [46,47]. For the trivial case of a non-grafted surface, no swelling occurs at the surface and, therefore,

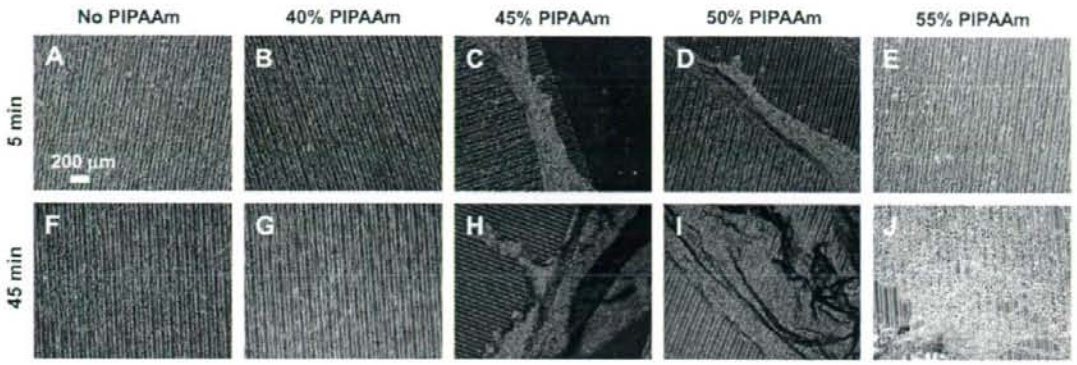

Fig. 3. Thermoresponsive cell sheet detachment is dependent on PIPAAm grafting density. The temperature of the cultures was dropped to 20 °C and observed at 5- (A–E) and 45-min (F–J) time points to assess cell detachment. Cell sheets grown on substrates without grafted PIPAAm (A, F) as well as those on 40% PIPAAm substrates (B, G) did not detach from the substrate within 45 min. Cell sheets grown on substrates made with 45% and 50% IPAAm began to detach within 5 min (C and D, respectively) and could be completely removed within 45 min (H and I, respectively). Sheets grown on substrates made with 55% IPAAm began to detach within 45 min, but did not detach as intact sheets (E, J).

no cell detachment occurs. At lower grafting densities (40% PIPAAm), the cells readily spread and grew on the surface but did not detach when the culture temperature was lowered to 20 °C. This is likely due to the fact that at lower grafting densities, most of the PIPAAm was tightly associated with the PS substrate and had limited chain mobility, which prevented the PIPAAm from swelling to the degree required to induce a disruption in adhesion [46]. At higher densities (45% and 50% PIPAAm), the swelling provided by the increased amount of grafted PIPAAm that was not tightly bound to the PS substrate was apparently sufficient to induce disruption. However, at still higher densities (55% PIPAAm), adhesion was disrupted but the cell sheets did not detach intact. In this case, it is possible that grafted PIPAAm layer did not fully support uniform cell adhesion and growth, resulting in poor cell sheet formation. It is interesting to note that these results indicate that there is an optimum range of PIPAAm grafting density for PS substrates made with the method described in this paper (45–50%) that is slightly lower than what is typically used to graft TCPS culture dishes (53–55%) [46]. Since both microtextured and non-microtextured exhibited optimal thermally-induced cell detachment in the same range of IPAAm concentration, it is unlikely that this difference is attributable to the microtexturing itself. The nature of the surface of the PS films used here may have been different than that of TCPS, potentially resulting in differences in PIPAAm grafting density and/or thickness between the two types of substrates. Given the sensitivity of thermally-induced cell detachment on the thickness of the grafted PIPAAm layer, even small differences in substrate surface chemistry could result in alterations to the functional thermoresponsive properties of the grafted substrates. Regardless of the mechanism, these results indicate that the optimum PIPAAm grafting density for cell sheet detachment must be determined whenever the substrate material is altered.

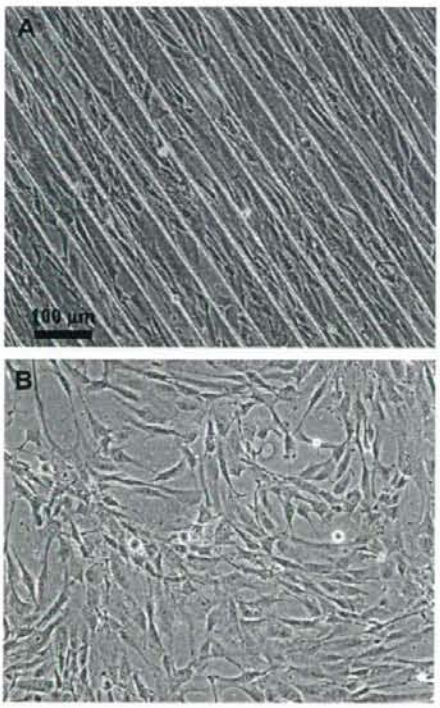

Fig. 4. Cell sheets grown on microtextured, PIPAAm-grafted substrates orient in direction of micropattern. Brightfield images of AoSMCs grown on microtextured PS substrates show that the cells oriented in the direction of the grooves (A), but oriented randomly on non-microtextured substrates (B). The substrates in these images were grafted with 45% PIPAAm.

Transferring mature cell sheets from patterned substrates onto non-patterned substrates, other cell sheets, and ultimately to the tissue/organ of interest for in vivo repair/regeneration is a crucial aspect of cell sheet technology. Additionally, for the organized cells such as the ones created here, this transfer must occur while maintaining the organization of the sheets, otherwise this method of generating cell sheets will be rendered useless if the organization is lost following detachment. Cell sheets tend to contract considerably when detached from PIPAAm-grafted substrates [23,48], which does not present a major problem for many applications employing isotropic cell sheets; however, in some cases it is desirable for the cell sheets to be used in their non-contracted form. For this reason, a simple method of sheet transfer has been previously developed [26]. Using a gelatin-coated stamp to aid in the detachment of the cell sheets, this method has been used to transfer cell sheets from one substrate to another while maintaining the original dimensions

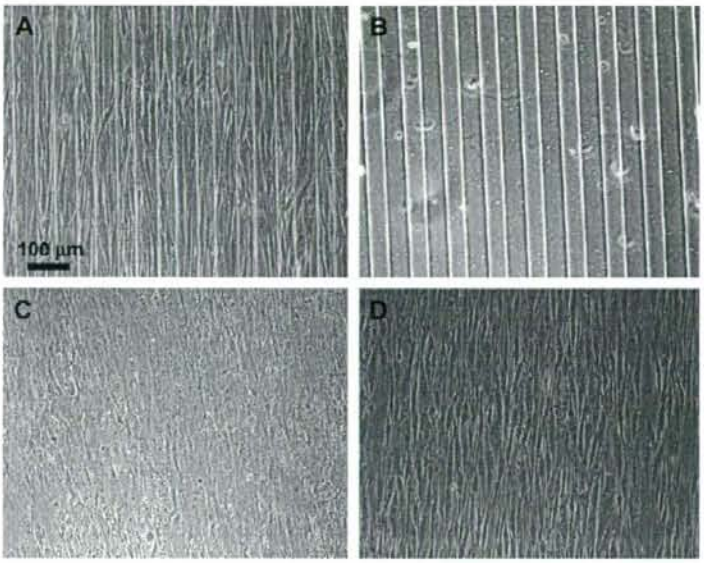

Fig. 5. Transferred cell sheets retain alignment. Cell sheets grown on thermoresponsive, microtextured substrates were transferred to non-textured TCPS culture dishes using a custom-built gelatin-coated manipulator (see text for details) without loss of cell orientation: an organized cell sheet on a microtextured 45% PIPAAm-grafted substrate (A), the microtextured PIPAAm substrate after cell sheet had been removed showing that no cells or matrix were left behind after detachment (B), the cell sheet attached to the gelatin-coated manipulator showing that the sheet remains organized following detachment (C), and the cell sheet attached to a non-patterned substrate post-transfer showing retention of cell/matrix organization.

of the sheets for the purpose of creating multilayer tissues comprising several stacked cell sheets. This method has been effectively utilized here for the transfer of organized cell sheets to TCPS culture dishes without loss of cell organization, as evidenced by the maintenance of cell angle distribution and F-actin organization. More recently, a method to generate tubular tissues from cell sheets has been developed [49], which is useful to the development of arterial tissue. This technique further expands the array of cell sheet

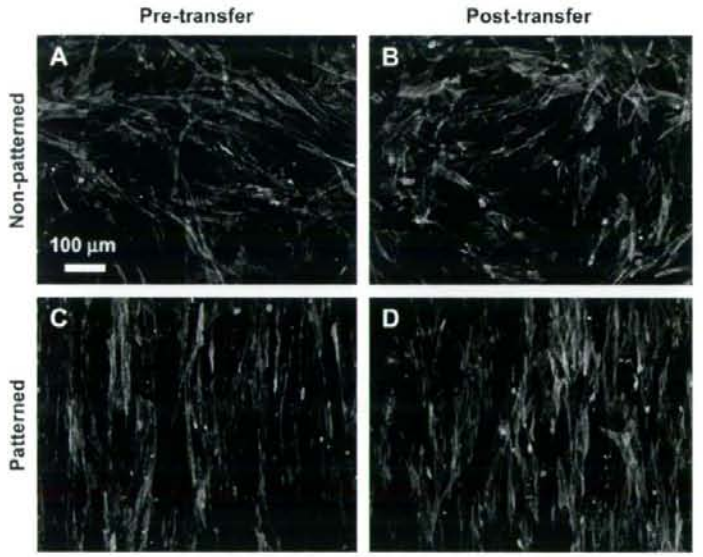

Fig. 6. Cell sheet cytoskeletal organization, pre- and post-transfer. Cytoskeletal organization of cell sheets was assessed by staining F-actin fibrils with Alexa Fluor 568 Phalloidin (Molecular Probes; 1:200 dilution). (A) Non-patterned, pre-transfer; (B) non-patterned, post-transfer; (C) patterned, pre-transfer; (D) patterned, post-transfer. In panels A and C (pre-transfer), cell sheets were still attached to PIPAAm-grafted PS substrates, while in panels B and D (post-transfer), the cell sheets have been transferred from PIPAAm-grafted substrates to TCPS.

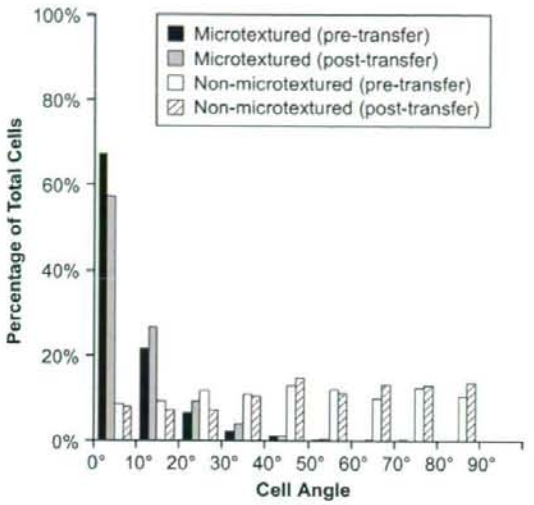

Fig. 7. Cell orientation distribution on microtextured and non-microtextured substrates, pre- and post-transfer. Cell orientation was quantified staining the cell nuclei of cells grown on substrates grafted with 45% PIPAAm with Hoechst 33342 for 30 min. For each individual substrate, five images were taken at random locations under epifluorescence and the cell orientation was measured by finding the angle between the long axis of the nuclei and the direction of the grooves. An angle of 0° indicated parallel orientation to the grooves, while an angle of 90° indicates a perpendicular orientation to the grooves. For non-microtextured substrates, the angle was arbitrarily chosen for each image. Cells grown on non-microtextured substrates (white bars) showed random distribution of cell orientation angles (no preferential orientation), while cells grown on microtextured substrates (black bars) showed a strong orientation response in the direction of the grooves. For both microtextured and non-microtextured substrates, the distribution of cell orientation angles did not change appreciably following transfer via the gelatin manipulator method (gray and hatched bars, respectively).

manipulation techniques that may be employed in order to form more complicated, multilayered organized tissues.

While these results are promising, considerable work remains in order to fully realize the potential of this system. The unique properties of tissues are strongly dictated by the quantity, composition, and organization of the ECM. As this study only focused on the short-term development of cell sheet on these substrates, we do not yet have any insight into the accumulation and organization of the cell-secreted matrix that will inevitably occur at longer times. It will be crucial to assess how the matrix is assembled as the sheets mature and whether the templating effect of the patterned substrates is maintained for long periods in culture as the sheets grow and thicken. Sheets retain their organization upon transfer to non-patterned surfaces, but the retention of this organization after an extended period in culture (weeks) has not been assessed. However, while cell and ECM organizations are crucial to producing a tissue with anisotropic properties, they are not measures of tissue performance in and of themselves. To this end, sophisticated, highly sensitive mechanical testing techniques [50] will be required in order to assess the mechanical anisotropy (or lack thereof) of such aligned tissues. Our preliminary investigations (not shown) indicate that such organization can lead to sheets with desired mechanical anisotropy. Lastly, combining multiple cell sheets via stacking or rolling is an essential aspect of cell sheet technology as it allows for creation of larger, more complicated tissues. While this has not been demonstrated for the organized cell sheets produced in this study, there is considerable evidence in the literature that sheets can be readily stacked into a number of configurations using many different cell types [17], including smooth muscle cells [51], suggesting that this should not present a major challenge. Future studies with these organized sheets will focus on creating multilayer tissues with a complete analysis of their morphological, biological, and mechanical properties.

While the work presented in this study was introduced within the framework of developing a tissue engineered vascular graft, we feel that this approach can be broadly applied to a number of tissue engineering applications where cell sheet engineering would be beneficial and precise structural control of the sheets is desired. Cardiac tissue engineering for infarct repair is currently one of the most highly studied applications for cell sheet engineering [17]. The cardiac wall comprises multiple layers of highly aligned cardiac muscle, which allows for enhanced cell–cell interactions and greatly improves contraction efficiency. Producing an aligned cardiac patch that could mimic the proper structure of the native cardiac wall and provide enhanced contractile function would likely be a dramatic improvement for infarct repair. Skeletal muscle engineering would likely receive the same benefits from such an aligned construct [52]. While the parallel groove pattern is well suited for the blood vessel and muscle applications, the patterning of these substrates is not limited to such simple geometries. Heart valve tissue engineering is one such area where complicated substrate patterning could be employed to improve tissue properties [53]. The unusual shape of the heart valve and complicated matrix organization make it a challenging target for tissue engineering. However, precise control of tissue structure offered by the technique described in this study may offer the ability to produce valve-like tissues with the desired organization. These are but a few possible examples of tissue engineering applications that could benefit from this technique.

5. Conclusions

In this study, we have described a simple, effective method of producing cell sheets with defined organization using thermoresponsive, microtextured substrates. The microtexturing provided guidance cues that allowed for the precise control of cellular organization, while the PIPAAm-coating facilitated harvest of intact cell sheets by means of a change in culture temperature. Furthermore, the patterned cell sheets retained their organization upon removal from the microtextured substrates, indicating that the microtexturing was not required to maintain the organization of the sheets. While only parallel groove patterns were investigated in this study, patterns are not limited to such simple geometries and can be as intricate as photolithographic techniques allow. We feel that this approach can be broadly applied to a number of tissue engineering applications where cell sheet engineering would be beneficial and precise structural control of the sheets is desired.

Acknowledgements

The authors would like to specifically acknowledge Masumi Yamada, Ph.D. and Megumi Muraoka for their technical assistance. This work has been supported by NIH (HL 72900) (J.Y.W.) and Formation of Innovation Center for Fusion of Advanced Technologies in the Special Coordination Funds for Promoting Science and Technology from the Ministry of Education, Culture, Sports, Science and Technology (MEXT), Japan (T.O.).

References

[1] Fung Y-C. Biomechanics: mechanical properties of living tissues. New York: Spinger-Verlag; 1993.
[2] Isenberg BC, Williams C, Tranquillo RT. Small-diameter artificial arteries engineered in vitro. Circ Res 2006;98(1):25–35.

[3] Teebken OE, Haverich A. Tissue engineering of small diameter vascular grafts. Eur J Vasc Endovasc Surg 2002;23(6):475–85.
[4] Schmedlen RH, Elbjeirami WM, Gobin AS, West JL. Tissue engineered small-diameter vascular grafts. Clin Plast Surg 2003;30(4):507–17.
[5] Canham PB, Talman EA, Finlay HM, Dixon JG. Medial collagen organization in human arteries of the heart and brain by polarized light microscopy. Connect Tissue Res 1991;26(1–2):121–34.
[6] Glagov S. Relation of structure to function in arterial walls. Artery 1979;5(4):295–304.
[7] Wolinsky H, Glagov S. Structural basis for the static mechanical properties of the aortic media. Circ Res 1964;14:400–13.
[8] Rhodin J. Architecture of the vessel wall. In: Berne R, editor. Handbook of physiology. Baltimore: Waverly Press, Inc.; 1980. p. 1–31.
[9] Barocas VH, Girton TS, Tranquillo RT. Engineered alignment in media equivalents: magnetic prealignment and mandrel compaction. J Biomech Eng 1998;120(5):660–6.
[10] L'Heureux N, Germain L, Labbe R, Auger FA. *In vitro* construction of a human blood vessel from cultured vascular cells: a morphologic study. J Vasc Surg 1993;17(3):499–509.
[11] Grassl ED, Oegema TR, Tranquillo RT. A fibrin-based arterial media equivalent. J Biomed Mater Res A 2003;66(3):550–61.
[12] Tower TT, Neidert MR, Tranquillo RT. Fiber alignment imaging during mechanical testing of soft tissues. Ann Biomed Eng 2002;30(10):1221–33.
[13] Isenberg BC, Williams C, Tranquillo RT. Endothelialization and flow conditioning of fibrin-based media-equivalents. Ann Biomed Eng 2006;34(6):971–85.
[14] L'Heureux N, McAllister TN, de la Fuente LM. Tissue-engineered blood vessel for adult arterial revascularization. N Engl J Med 2007;357(14):1451–3.
[15] Grenier G, Remy-Zolghadri M, Larouche D, Gauvin R, Baker K, Bergeron F, et al. Tissue reorganization in response to mechanical load increases functionality. Tissue Eng 2005;11(1–2):90–100.
[16] Auger FA, Remy-Zolghadri M, Grenier G, Germain L. The self-assembly approach for organ reconstruction by tissue engineering. e-Biomed: J Regen Med 2000;1(5):75–86.
[17] Yang J, Yamato M, Shimizu T, Sekine H, Ohashi K, Kanzaki M, et al. Reconstruction of functional tissues with cell sheet engineering. Biomaterials 2007;28(34):5033–43.
[18] Okano T, Yamada N, Okuhara M, Sakai H, Sakurai Y. Mechanism of cell detachment from temperature-modulated, hydrophilic–hydrophobic polymer surfaces. Biomaterials 1995;16(4):297–303.
[19] Heskins M, Guilent JE, James E. Solution properties of poly(*N*-isopropylacrylamide). J Macromol Sci A 1968;2(8):1441–55.
[20] Canavan HE, Cheng X, Graham DJ, Ratner BD, Castner DG. Cell sheet detachment affects the extracellular matrix: a surface science study comparing thermal liftoff, enzymatic, and mechanical methods. J Biomed Mater Res A 2005;75(1):1–13.
[21] Kushida A, Yamato M, Isoi Y, Kikuchi A, Okano T. A noninvasive transfer system for polarized renal tubule epithelial cell sheets using temperature-responsive culture dishes. Eur Cell Mater 2005;10:23–30. discussion 23–30.
[22] Kushida A, Yamato M, Kikuchi A, Okano T. Two-dimensional manipulation of differentiated Madin-Darby canine kidney (MDCK) cell sheets: the noninvasive harvest from temperature-responsive culture dishes and transfer to other surfaces. J Biomed Mater Res 2001;54(1):37–46.
[23] Kushida A, Yamato M, Konno C, Kikuchi A, Sakurai Y, Okano T. Decrease in culture temperature releases monolayer endothelial cell sheets together with deposited fibronectin matrix from temperature-responsive culture surfaces. J Biomed Mater Res 1999;45(4):355–62.
[24] Canavan HE, Cheng X, Graham DJ, Ratner BD, Castner DG. Surface characterization of the extracellular matrix remaining after cell detachment from a thermoresponsive polymer. Langmuir 2005;21(5):1949–55.
[25] Tsuda Y, Kikuchi A, Yamato M, Nakao A, Sakurai Y, Umezu M, et al. The use of patterned dual thermoresponsive surfaces for the collective recovery as co-cultured cell sheets. Biomaterials 2005;26(14):1885–93.
[26] Tsuda Y, Shimizu T, Yamato M, Kikuchi A, Sasagawa T, Sekiya S, et al. Cellular control of tissue architectures using a three-dimensional tissue fabrication technique. Biomaterials 2007;28(33):4939–46.
[27] Desai TA. Micro- and nanoscale structures for tissue engineering constructs. Med Eng Phys 2000;22(9):595–606.
[28] Curtis A, Wilkinson C. Topographical control of cells. Biomaterials 1997;18(24):1573–83.
[29] Kane RS, Takayama S, Ostuni E, Ingber DE, Whitesides GM. Patterning proteins and cells using soft lithography. Biomaterials 1999;20(23–24):2363–76.
[30] Thakar RG, Ho F, Huang NF, Liepmann D, Li S. Regulation of vascular smooth muscle cells by micropatterning. Biochem Biophys Res Commun 2003;307(4):883–90.
[31] Chen CS, Mrksich M, Huang S, Whitesides GM, Ingber DE. Micropatterned surfaces for control of cell shape, position, and function. Biotechnol Prog 1998;14(3):356–63.
[32] Dusseiller MR, Schlaepfer D, Koch M, Kroschewski R, Textor M. An inverted microcontact printing method on topographically structured polystyrene chips for arrayed micro-3-D culturing of single cells. Biomaterials 2005;26(29):5917–25.
[33] Feng J, Chan-Park MB, Shen JY, Chan V. Quick layer-by-layer assembly of aligned multilayers of vascular smooth muscle cells in deep microchannels. Tissue Eng 2007;13(5):1003–12.
[34] Sarkar S, Dadhania M, Rourke P, Desai TA, Wong JY. Vascular tissue engineering: microtextured scaffold templates to control organization of vascular smooth muscle cells and extracellular matrix. Acta Biomater 2005;1(1):93–100.
[35] Wilkinson CD. Making structures for cell engineering. Eur Cell Mater 2004;8:21–5. discussion 25–26.
[36] Vernon RB, Gooden MD, Lara SL, Wight TN. Microgrooved fibrillar collagen membranes as scaffolds for cell support and alignment. Biomaterials 2005;26(16):3131–40.
[37] Charest JL, Bryant LE, Garcia AJ, King WP. Hot embossing for micropatterned cell substrates. Biomaterials 2004;25(19):4767–75.
[38] Boland T, Xu T, Damon B, Cui X. Application of inkjet printing to tissue engineering. Biotechnol J 2006.
[39] Odde DJ, Renn MJ. Laser-guided direct writing of living cells. Biotechnol Bioeng 2000;67(3):312–8.
[40] Pins GD, Bush KA, Cunningham LP, Campagnola PJ. Multiphoton excited fabricated nano and micro patterned extracellular matrix proteins direct cellular morphology. J Biomed Mater Res A 2006;78(1):194–204.
[41] Xia Y, Whitesides G. Soft lithography. Ann Rev Mater Sci 1998;28(1):153–84.
[42] Russo AP, Apoga D, Dowell N, Shain W, Turner AMP, Craighead HG, et al. Microfabricated plastic devices from silicon using soft intermediates. Biomed Microdevices 2002;4(4):277–83.
[43] Yamada N, Okano T, Sakai H, Karikusa F, Sawasaki Y, Sakurai Y. Thermoresponsive polymeric surfaces – control of attachment and detachment of cultured-cells. Makromol Chem-Rapid 1990;11(11):571–6.
[44] Dunn GA. Contact guidance of cultured tissue cells: a survey of potentially relevant properties of the substratum. In: Bellairs ACR, Dunn G, editors. Cell Behaviour. Cambridge: Cambridge University Press; 1982. p. 247–80.
[45] Tsuda Y, Kikuchi A, Yamato M, Chen G, Okano T. Heterotypic cell interactions on a dually patterned surface. Biochem Biophys Res Commun 2006;348(3):937–44.
[46] Akiyama Y, Kikuchi A, Yamato M, Okano T. Ultrathin poly(*N*-isopropylacrylamide) grafted layer on polystyrene surfaces for cell adhesion/detachment control. Langmuir 2004;20(13):5506–11.
[47] Cheng X, Canavan HE, Stein MJ, Hull JR, Kweskin SJ, Wagner MS, et al. Surface chemical and mechanical properties of plasma-polymerized *N*-isopropylacrylamide. Langmuir 2005;21(17):7833–41.
[48] Kwon OH, Kikuchi A, Yamato M, Sakurai Y, Okano T. Rapid cell sheet detachment from poly(*N*-isopropylacrylamide)-grafted porous cell culture membranes. J Biomed Mater Res 2000;50(1):82–9.
[49] Kubo H, Shimizu T, Yamato M, Fujimoto T, Okano T. Creation of myocardial tubes using cardiomyocyte sheets and an in vitro cell sheet-wrapping device. Biomaterials 2007;28(24):3508–16.
[50] Black LD, Brewer KK, Morris SM, Schreiber BM, Toselli P, Nugent MA, et al. Effects of elastase on the mechanical and failure properties of engineered elastin-rich matrices. J Appl Physiol 2005;98(4):1434–41.
[51] Yang J, Yamato M, Kohno C, Nishimoto A, Sekine H, Fukai F, et al. Cell sheet engineering: recreating tissues without biodegradable scaffolds. Biomaterials 2005;26(33):6415–22.
[52] Rowlands AS, Hudson JE, Cooper-White JJ. From scrawny to brawny: the quest for neomusculogenesis; smart surfaces and scaffolds for muscle tissue engineering. Exp Rev Med Devices 2007;4(5):709–28.
[53] Mendelson K, Schoen FJ. Heart valve tissue engineering: concepts, approaches, progress, and challenges. Ann Biomed Eng 2006;34(12):1799–819.

Available online at www.sciencedirect.com
ScienceDirect
Biomaterials 29 (2008) 2073–2081
Biomaterials
www.elsevier.com/locate/biomaterials

Preparation of thermoresponsive polymer brush surfaces and their interaction with cells

Aya Mizutani [a], Akihiko Kikuchi [b,1], Masayuki Yamato [b], Hideko Kanazawa [a], Teruo Okano [b,*]

[a] Department of Pharmacy, Kyoritsu University of Pharmacy, 1-5-14 Shibakoen, Minato, Tokyo 105-0011, Japan
[b] Institute of Advanced Biomedical Engineering and Science, Center of Excellence for the 21st Century, Tokyo Women's Medical University, 8-1 Kawadacho, Shinjuku, Tokyo 162-8666, Japan

Received 16 October 2007; accepted 13 January 2008
Available online 7 February 2008

Abstract

Poly(*N*-isopropylacrylamide) (PIPAAm) brush surfaces with different layer thickness on polystyrene substrates were prepared by surface-initiated atom transfer radical polymerization (ATRP). Surface characteristics of PIPAAm brushes and their influence on adhesion and detachment of bovine carotid artery endothelial cells (ECs) were controlled by PIPAAm layer thickness. Surface hydrophilicity increased with PIPAAm layer thickness at 37 °C because PIPAAm brush surfaces with higher thickness provide more extended chain conformations with relatively high chain mobility, and accompanying polymer chain hydration. These surface property alterations lead to negligible cell adhesion through minimal matrix protein adsorption and also modified surface modulus. By adjusting polymerization reaction conditions and time, polymer layers supporting confluent cultures of ECs were possible. Confluent EC monolayers spontaneously detached as contiguous cell sheets from PIPAAm brush surfaces at reduced temperatures. Thermoresponsive cell adhesion and detachment behavior were analyzed from the standpoint of surface physicochemical characteristics. Thermoresponsive surfaces prepared by surface-initiated ATRP techniques allow surface selection in preparing cell sheets from attachment-dependent cells having relatively strong adhesive property for tissue engineering applications.

Keywords: Thermoresponsive polymer; Poly(*N*-isopropylacrylamide); Atom transfer radical polymerization; Cell culture; Polystyrene substrates

1. Introduction

Intelligent interfaces are currently recognized as valuable new materials with novel properties relevant for biomedical research fields such as artificial organs, biofunctional materials, drug delivery systems, separation of biomolecules, and regenerative medicine, respectively. We developed novel intelligent surfaces with reversible hydrophilic/hydrophobic surface property alterations in response to external thermal stimuli [1–5]. Thermoresponsive polymers, poly(*N*-isopropylacrylamide) (PIPAAm) and its derivatives, are commonly used as surface modifiers [1–5]. PIPAAm is soluble with a hydrated, extended chain conformation in aqueous solution below 32 °C and becomes insoluble due to rapid, reversible chain dehydration and aggregation above this temperature [6,7]. Thermoresponsive PIPAAm surface property alterations allow modulation of molecular interactions with surfaces as a function of temperature for chromatographic separations of bioactive molecules [4,5,8]. In addition, we have been able to regulate adhesion and detachment of cultured cells using only temperature modulation [1–3]. We further demonstrated recovery of confluently cultured cells as contiguous intact cell sheets by low temperature treatment [9,10]. This has been recently extended to a cell-based therapy for patients with severe disorders of the cornea using living cornea epithelial cell sheets and/or oral mucosal epithelial cell sheets harvested from thermoresponsive culture dishes [11,12]. We also demonstrated cell sheet-based possibilities for esophagus epithelium transplantation [13], and periodontal ligament transplantation [14].

* Corresponding author. Fax: +81 3 3359 6046.
E-mail address: tokano@abmes.twmu.ac.jp (T. Okano).
[1] Present address: Department of Materials Science and Technology, Tokyo University of Science, 2641 Yamazaki, Noda, Chiba 278-8510, Japan.

0142-9612/$ - see front matter © 2008 Elsevier Ltd. All rights reserved.
doi:10.1016/j.biomaterials.2008.01.004

Our postulated mechanism for thermally regulated cell adhesion/detachment on PIPAAm grafted surfaces involves thermally regulated cell detachment based on cellular metabolic activity requiring ATP consumption [2,15,16]. Temperature reduction promotes polymer layer hydration, softening, loss of local mechanical modulus and also cell-surface receptor engagement. Cultured cells are recovered together with most of their deposited extracellular matrix (ECM) proteins such as fibronectin (FN), laminin, and collagen [17–20] and maintain cell-to-cell junctions in monolayer cell sheet recovery [21]. Adherent cellular traction forces are lost upon polymer hydration but receptors keep attached to ECM and remove it from the surface. Furthermore, PIPAAm grafted layer thickness is known to influence cell adhesion and FN adsorption [18].

To date, many studies have reported the preparation of PIPAAm films for cell related experiments including surfaces prepared by electron beam (EB) irradiated polymerization with a cross-linked thin hydrogel structure [3,18], a plasma-deposited PIPAAm film [19,20], PIPAAm hydrogels [22], air-dried PIPAAm gelatin mixtures [23], PIPAAm-collagen mixtures that are UV irradiated [24], etc. However, in such polymer film preparations, grafted molecular density, length, crosslinking, and chain motion of the polymer on the supporting surfaces are not defined. As chain properties define both the local mechanical and thermal-hydration characteristics and dynamics of the polymer layer, it is important to analyze the effects of polymer chain configurations of thermoresponsive surfaces on cell adhesion/detachment behavior with temperature.

A relatively new polymerization technique called living radical polymerization (LRP), has been extensively investigated [25]. Dense polymer grafted surfaces with controlled polymer layer thickness (polymer brush surfaces) can be prepared by atom transfer radical polymerization (ATRP), a highly investigated LRP technique. Many peculiar characteristics of "polymer brushes" prepared by ATRP have been reported. Wu et al. [26] prepared polyacrylamide brush surfaces on silica and showed grafted polymer chains were highly extended. Xiao and Wirth prepared polyacrylamide brush surfaces on silica [27] or poly(dimethylsiloxane) [28] and found resistance to irreversible protein adsorption [27,28]. We have already prepared PIPAAm brush surfaces on glass [29] or silica beads [30] and applied these to several separation systems [29,30]. Other researchers also have reported the preparation of PIPAAm brush by ATRP. Balamurugan et al. [31] and Shan et al. [32] independently prepared PIPAAm brush surfaces on gold and investigated thermoresponsive hydration transition behavior. Xu et al. [33] prepared PIPAAm brush surfaces on silicon and observed 3T3 adhesion/detachment behavior according to the temperature changes.

In the present contribution, we describe design and preparation of densely grafted PIPAAm brush surfaces using surface-initiated ATRP to investigate relationships between surface characteristics and cultured cell adhesion/detachment behavior. We found that grafted PIPAAm layer thickness and amounts greatly influenced cell adhesion/detachment behavior analogous to that on cross-linked PIPAAm grafted surfaces prepared by EB polymerization method [18]. In addition, cell adhesion/detachment control was possible even though the polymer amount was smaller than the previous cross-linked PIPAAm grafted surfaces [18]. As radiation and plasma grafting methods suffer from batch-to-batch variability and substrate-dependent issues from our experience, such polymer brush surfaces should be valuable for modulation of cell adhesion/detachment for further development of cell sheet-based regenerative medicine.

2. Materials and methods

2.1. Materials

N-isopropylacrylamide (IPAAm) was kindly provided by Kohjin (Tokyo, Japan) and purified by recrystallization from *n*-hexane, followed by thorough drying in vacuo at 25 °C. Polystyrene dishes (Falcon 1007) and tissue culture polystyrene dishes (TCPS, Falcon 3002) were both obtained from BD Bioscience (Billerica, MA, USA). Polystyrene dishes (Falcon 1007) were cut with an ultrasonic cutter (SUW-30CTL, SUZUKI, Shizuoka, Japan) to create rectangular substrates (2.4 cm-wide × 7.6 cm-long). 4-Vinylbenzyl chloride was obtained from Fluka (Deisenhofen, Germany). Dehydrated toluene, 2,2′-zobis(isobutyronitrile) (AIBN), and dimethylsulfoxide (DMSO) were purchased from Wako Pure Chemicals Industries Co. Ltd. (Osaka, Japan). Tris(2-aminoethyl)amine was obtained from Acros Organics (Pittsburgh, PA, USA). Formaldehyde, formic acid, sodium hydroxide, chloroform, and anhydrous magnesium sulfate were purchased from Wako Chemicals. Copper (I) chloride (CuCl), copper (II) chloride ($CuCl_2$), methanol, and acetone were obtained from Wako Chemicals. Bovine carotid artery endothelial cells (ECs) were obtained from Health Science Research Resources Bank (Osaka, Japan). Dulbecco's modified Eagle's medium (DMEM), penicillin–streptomycin solution (100 unit/ml penicillin, and 100 μg/ml streptomycin), Dulbecco's phosphate buffered saline (D-PBS), and trypsin–EDTA solution, were purchased from Sigma Chemicals (St. Louis, MO, USA). Fetal bovine serum (FBS; Mexico origin) was obtained from Bioserum Co. Ltd. (Victoria, Australia). Rhodamine-labelled fibronectin (FN) from bovine plasma (freeze dried from 1.0 mg/ml in 50 mM Tris–HCl pH 7.5 plus 0.5 M NaCl) was obtained from Cytoskeleton (Denver, CO, USA).

2.2. Preparation of ATRP initiator-modified polystyrene surfaces

To prepare the ATRP initiator, 4-vinylbenzyl chloride was polymerized by conventional radical polymerization. Solutions containing 4-vinylbenzyl chloride (50 mL, 0.35 mol) and AIBN (164.2 mg, 1.0 mmol) as an initiator were prepared in 100 mL toluene. The reaction mixture was degassed by triplicate freeze–thaw cycles, and the flask was sealed under reduced pressure. Polymerization then proceeded at 70 °C for 20 h. After the reaction solution was concentrated by evaporation, polymer solution was poured into methanol to precipitate the polymer. The polymer was further purified by repeated precipitation from acetone into methanol twice and then dried at 25 °C for overnight under vacuum. Poly(4-vinylbenzyl chloride) was dissolved in DMSO (3 w/w%) and deposited on polystyrene substrates (2.4 cm-wide × 7.6 cm-long) using a spin coater (ACT-300D, ACTIVE Co., Ltd., Saitama, Japan) at 1000 rpm for 30 s. Prepared ATRP initiator-modified surfaces were dried at 45 °C for overnight under vacuum.

2.3. Preparation of PIPAAm brush surfaces

PIPAAm brush surfaces were prepared by surface-initiated ATRP on initiator-modified polystyrene surfaces [25,29] in aqueous solution. Tris(2-dimethylaminoethyl)amine (Me_6TREN) as an ATRP ligand was synthesized using a previously reported method [29,34]. Ultrapure water (Milli-Q water)

obtained using Milli-Q Synthesis (Millipore, Billerica, MA, USA) (500 mL) was used as solvent and deoxygenated with nitrogen gas bubbling for 2 h at 25 °C. IPAAm monomer, CuCl 148.5 mg (1.5 mmol), $CuCl_2$ 20.2 mg (150 μmol), Me_6TREN 412.8 μl (1.5 mmol), and initiator-modified polystyrene surfaces installed in a separable flask were placed into a glove box. Initial IPAAm concentration was changed as 566 mg (5 mmol), 11.3 g (100 mmol), and 17.0 g (150 mmol), respectively. The glove box was then degassed and flushed three times with nitrogen gas. IPAAm, CuCl, $CuCl_2$, and Me_6TREN were dissolved in Milli-Q water, and the reaction solution was then poured into initiator-modified polystyrene surfaces installed in the separable flask. The ATRP reaction proceeded at 25 °C inside the glove box for predetermined time period under gentle stirring. PIPAAm brush surfaces were rinsed repeatedly with Milli-Q water and methanol, and then dried at 25 °C overnight under vacuum. Preparation of PIPAAm brushes on polystyrene surfaces is schematically shown in Scheme 1. PIPAAm brush surfaces are abbreviated as brush-X–Y where X is initial IPAAm concentration in mM, and Y is reaction time in hours.

2.4. XPS analysis of PIPAAm brush surfaces

Elemental analysis was performed for brush-300–0.5 and ATRP initiator-modified surfaces as reference surfaces by X-ray photoelectron spectroscopy (XPS; Quantera SXM, Physical Electronics, Chanhassen, MN, USA). All the XPS measurements were performed by the Toray Research Center, Inc. (Tokyo, Japan). Excitation X-rays were produced from a monochromatic Al $K\alpha_{1,2}$ source with a beam diameter of 100 μm, and take-off angle of 15°. (The effective escape depth for photoelectron was ca. 2.5 nm.) Wide scans were recorded to analyze all existing elements on the surfaces, and high resolution narrow scan analysis was performed for peak deconvolution of carbon C1s signals. All binding energies were referenced to the C1s hydrocarbon peak at 284.6 eV.

2.5. Thermoresponsive wettability changes of PIPAAm brush surfaces

Thermoresponsive surface wettability was evaluated by static contact angle measurement (Image processing type CA-X, Kyowa Interface Science Co., Ltd., Saitama, Japan) using captive bubble method. Sample specimen was immersed in Milli-Q water in quartz cells and contact angle was measured after placing the air bubble onto the sample surfaces. Sample temperature was regulated with a circulating water bath (Thermo Controller 4VF, Kyowa Interface Science Co., Ltd.) within ±0.1 °C. Data are expressed as the mean of three measurements with standard deviation (SD).

2.6. Amount of grafted PIPAAm

Amount of grafted PIPAAm was determined by attenuated total reflection Fourier transform infrared spectroscopy (ATR/FTIR, Spectrum One, PerkinElmer, Waltham, MA, USA) using germanium as an ATR crystal (GATR, Harrick Scientific Corporation, Pleasantville, NY, USA). As the base substrate was polystyrene, an absorption arising from mono-substituted aromatic rings was observed at 1600 cm^{-1}. Absorption of amide carbonyl (amide I) derived from PIPAAm side groups appeared in the region of 1650 cm^{-1}. The peak intensity ratio of I_{1650}/I_{1600} was used to determine amounts of grafted PIPAAm on surfaces. A known PIPAAm amount cast on polystyrene from solution was used to prepare a calibration curve. Data are expressed as the mean of four measurements with SD.

2.7. PIPAAm grafted layer thickness

Ellipsometric measurements of the PIPAAm layer thickness in dry state were made on an M-2000D instrument (J.A. Woollam Co., Inc., Lincoln, NE, USA) at wavelengths ranging from 193 to 1000 nm. The values of amplitude ratio, Ψ, and phase difference, Δ, of polarized light (p polarization and s polarization) from sample surfaces are measured. The values of Ψ and Δ are related to the ratio of Fresnel's amplitude reflection coefficients, R_p, and R_s, for p polarization and s polarization expressed in Eq. (1):

$$\rho = R_p/R_s = \tan(\Psi)e^{i\Delta} \tag{1}$$

where ρ is the complex reflectance ratio. Measured Ψ and Δ were converted into optical constants and layer thickness by fitting to the function model using WVASE32 software (J.A. Woollam Co., Inc.).

2.8. Cell culture

ECs were cultured on conventional TCPS dishes in DMEM supplemented with 10% FBS, 100 unit/ml penicillin, and 100 μg/ml streptomycin at 37 °C in a humidified atmosphere with 5.0% CO_2. ECs were recovered from conventional TCPS dishes by treatment with 0.1% trypsin containing 1.1 mM EDTA in PBS. Recovered single cells were seeded on PIPAAm brush surfaces having different amounts of grafted PIPAAm, ATRP initiator-modified surfaces, and TCPS dishes as a reference, at 1.0×10^4 cells/cm^2 for observation of EC adhesion and detachment, and at 1.0×10^5 cells/cm^2 for preparing EC monolayer sheets. All of these surfaces were connected firmly with silicone gaskets (2.4 cm × 2.4 cm × thickness 8 mm) having a circular hole of 2 cm diameter. EC suspensions were poured into circular holes (culture area of 3.1 cm^2) (Fig. 1) and cultured on PIPAAm brush surfaces at 37 °C in a humidified atmosphere of 5% CO_2 for 24 h, and then transferred to the incubator set at 20 °C and again incubated for 2 h to determine both cell adhesion and detachment. Cell morphology was photographed at predetermined times under a phase-contrast microscope (ECLIPSE TE2000-U, Nikon, Tokyo, Japan) equipped with a digital camera (FinePix S2Pro, FUJIFILM, Tokyo, Japan). Adhered ECs were counted randomly on the microphotographs in multiple areas. Percent cell adhesion was then calculated as the mean of four measurements with SD. Furthermore, we examined confluent culture of ECs on brush-200–0.5 at 37 °C for 3 days, and then incubated at 20 °C for 1 h to determine recovery of ECs.

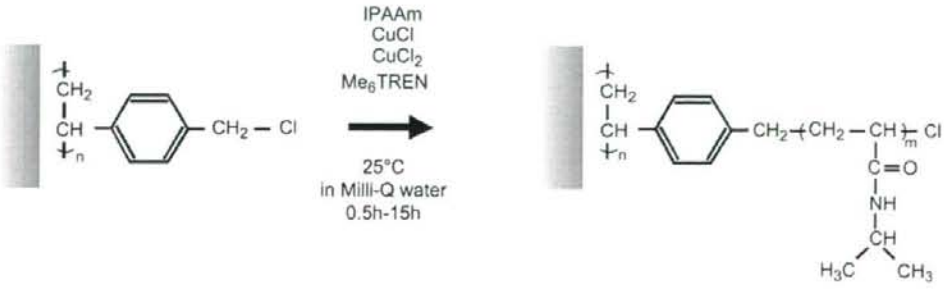

Scheme 1. Preparation of PIPAAm grafted surfaces via surface-initiated ATRP technique.

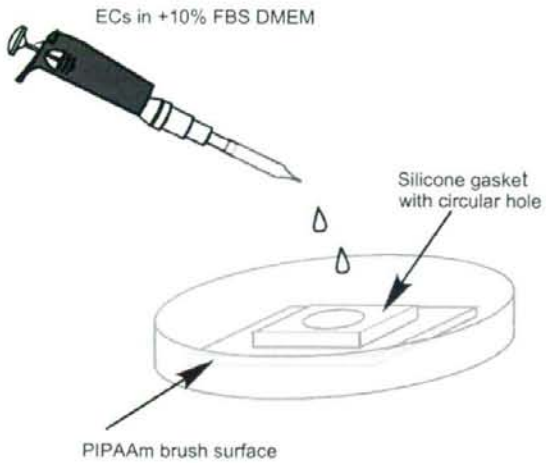

Fig. 1. Experimental procedure of cell culture on PIPAAm brush surfaces. PIPAAm grafted surfaces were connected with silicone gasket with circular holes (2 cm in diameter) and placed in PSt dishes.

2.9. FN adsorption onto PIPAAm brush surfaces

Rhodamine-labelled FN was used to examine FN adsorption onto PIPAAm brush surfaces having different amounts of grafted PIPAAm. FN adsorption was carried out by incubation of PIPAAm dishes with 10 μg/ml Rhodamine-labelled FN in D-PBS solution at 37 °C for 1 h. These dishes were then washed with D-PBS for three times at 37 °C. Finally, these dishes were observed under fluorescence microscopy (ECLIPSE TE2000-U, Nikon) and data were collected with AxioVision (version 3.1) (Carl Zeiss, Inc., NY, USA).

3. Results and discussion

3.1. Preparation of PIPAAm brush surfaces by ATRP

PIPAAm grafted surfaces were prepared by surface-initiated ATRP from surface coated poly(4-vinylbenzyl chloride). XPS measurements were carried out on PIPAAm grafted surfaces. Table 1 summarizes elemental composition of PIPAAm brush surfaces. Brush-300−0.5 was rich in N and C−N structure in comparison with ATRP initiator-modified surfaces. Nitrogen to carbon ratio of the brush-300−0.5 (N/C = 0.16) was comparable to the calculated value for theoretical chemical composition of IPAAm (N/C = 0.17). Moreover, satellite peaks (292 eV) originating from aromatic ring chemistry observed on ATRP initiator-coated surfaces (Fig. 2a), did not appear on brush-300−0.5 (Fig. 2b). Thus, the polystyrene substrate was not exposed on the interfaces of brush-300−0.5. These results indicate the successful polymerization of PIPAAm on ATRP initiator-modified polystyrene substrata.

The amount of grafted PIPAAm on prepared surfaces with fixed monomer concentration of 300 mM with various reaction times were determined by ATR/FTIR measurements [18]. Fig. 3 shows changes in the grafted PIPAAm amounts with reaction time. Amount of grafted PIPAAm increased with reaction time and leveled off around 10 h. Generation of radicals in ATRP is induced by reversible oxidation of the transition metal complexes in catalyst system and halogens at chain ends, thus polymer chains grow similarly to conventional radical polymerization [25]. The principle of the ATRP relies on the equilibrium between dormant and active chain ends, with the equilibrium preferring the dormant species. It leads to elimination of termination reactions, lowering polydispersity and enabling control of molecular weight [25,35]. Moreover, in ATRP, molecular weight increases linearly with conversions [25]. As can be seen in Fig. 3, PIPAAm grafted amount on the surfaces increased linearly for up to 10 h-reaction, illustrating its mechanism of ATRP.

3.2. Characterization of PIPAAm brush interfaces

Surface-grafted PIPAAm transition temperatures for brush-300−0.5 were determined by static contact angles in Milli-Q water. Fig. 4 shows static contact angle changes with temperature, ranging from 20 to 50 °C for brush-300−0.5 and for ATRP initiator-modified surfaces. Brush-300−0.5 showed relatively hydrophilic nature below 32 °C and became hydrophobic above this temperature, while initiator-modified surfaces were hydrophobic regardless of temperature. The result agreed with the previous reports [29,31]. Contact angle measurement is sensitive to the outermost region of grafted PIPAAm having the most significant influence on cell adhesion. That is, outermost region of grafted PIPAAm showed a sharp property change at 32 °C. Detailed discussion about the phase transition behavior of PIPAAm brush surfaces will be discussed later.

Table 1
Elemental analyses and peak deconvolution of XPS carbon C1s peaks on PIPAAm brush surfaces take-off angle of 15°, the effective escape depth for photoelectron was ca. 2.5 nm

Sample	Element (atom %)				N/C	Peak deconvolution of C1s peaks (%)			
	C	N	O	Cl		C−C, C−Hx[a]	C−Cl, C−N[b]	C=O[c]	Satellite peak[d]
Initiator-modified	91.6	0.3	3.3	4.8	<0.01	85	10	<1	4
Brush-300−0.5	76.3	12.0	11.5	0.2	0.16	62	22	16	–
Calcd.	75.0	12.5	12.5	–	0.17	66.7	16.7	16.7	–

[a] Binding energy of C−C and C−Hx are 284.6.
[b] C−Cl and C−N are 286.2.
[c] C=O is 287.6.
[d] Satellite peak is 291.2 eV, respectively.

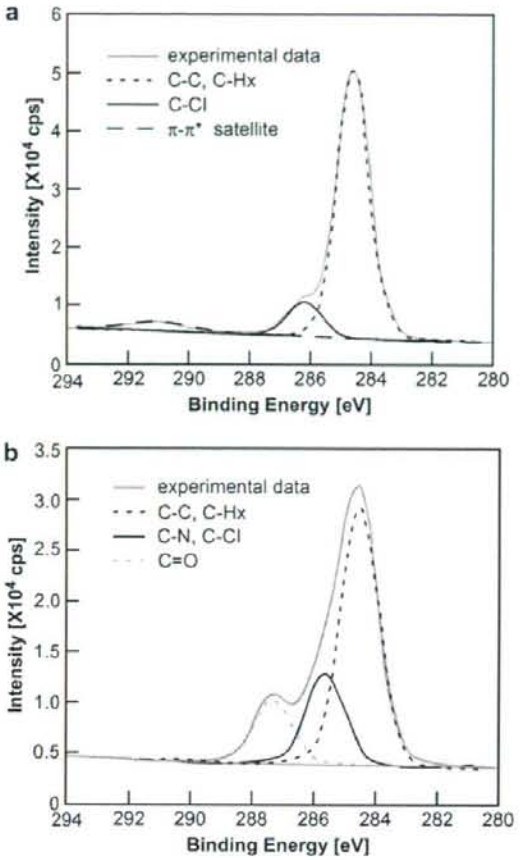

Fig. 2. Peak deconvolution of XPS carbon C1s peaks for (a) ATRP initiator-modified surfaces and (b) brush-300−0.5, showing the different carbon components on the surface.

Surface characterization of PIPAAm brush surfaces prepared by changing polymerization conditions was summarized in Table 2. We evaluated PIPAAm layer dry thickness by ellipsometric measurements of PIPAAm brush surfaces. Surfaces have a total of three layers of base polystyrene, poly(4-vinylbenzyl chloride) as ATRP initiator layer, and the PIPAAm grafted surfaces. Observed refractive indices of PSt substrate, PSt coated with poly(4-vinlbenzyl chloride) and PIPAAm brush surfaces at 589 nm wavelength (Sodium D line) were 1.582 (document value, $n = 1.59-1.60$ [36]), 1.595 and 1.490, respectively. PIPAAm layer thickness was summarized in Table 2. PIPAAm layer thickness for brush-10−1, brush-200−0.5, brush-300−0.5 and brush-300−6 were 1.8, 10.9, 30.4 and 64.7 nm, respectively. These results indicate that PIPAAm layer thickness increased with the grafted amount of PIPAAm. In addition, surface hydrophilicity increased with the amount of PIPAAm at both 20 and 37 °C, as can be seen in Table 2.

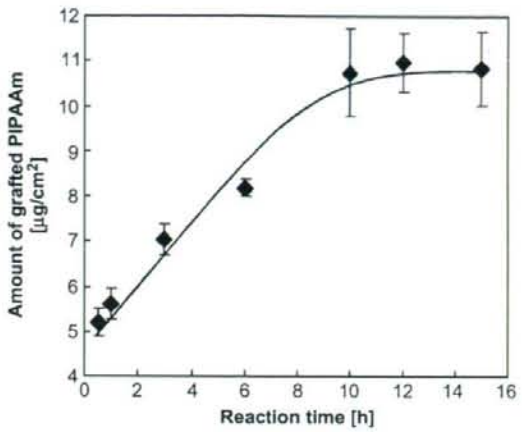

Fig. 3. Time course for amounts of grafted PIPAAm for PIPAAm brush surfaces prepared by fixed monomer concentration of 300 mM. Data from four separate experiments are expressed as mean ± SD.

3.3. Cell adhesion/detachment behavior

Six types of thermoresponsive surfaces were used for cell culture experiments. ECs were cultured on these surfaces for 24 h at 37 °C and then transferred to the incubator set at

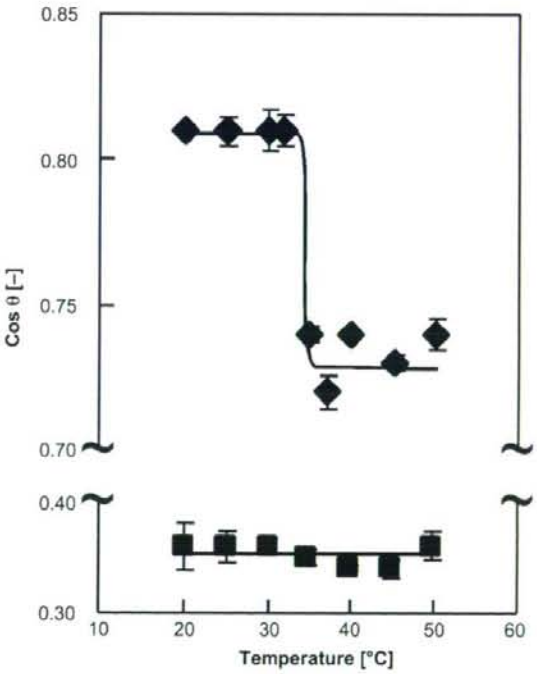

Fig. 4. Temperature-dependent contact angle changes for brush-300−0.5 (diamond symbols) and ATRP initiator-modified surface (square symbols) used as control surfaces. Data from three separate experiments are shown as mean ± SD.

Table 2
Amounts of surface-grafted PIPAAm and static contact angles for PIPAAm brush surfaces

Sample	Amount of grafted PIPAAm ($\mu g/cm^2$)[a]	PIPAAm dry layer thickness (nm)[b]	Contact angle ($\cos\theta$)[c]	
			37 °C	20 °C
Brush-10−1	0.4 ± 0.1	1.8	0.60 ± 0.01	0.66 ± 0.01
Brush-200−0.5	2.1 ± 0.2	10.9	0.70 ± 0.01	0.75 ± 0.01
Brush-300−0.5	5.2 ± 0.3	30.4	0.72 ± 0.01	0.79 ± 0.00
Brush-300−1	5.6 ± 0.3	36.9	0.74 ± 0.01	0.82 ± 0.01
Brush-300−3	7.9 ± 0.3	50.7	0.74 ± 0.01	0.85 ± 0.00
Brush-300−6	8.2 ± 0.2	64.7	0.81 ± 0.00	0.87 ± 0.00

[a] Data from four separate experiments are shown as mean ± SD.
[b] Measured by ellipsometry.
[c] Determined by captive bubble methods in water. Data from three separate experiments with SD.

20 °C and again incubated for 2 h to determine thermoresponsive cell adhesion and detachment [1,3]. Fig. 5 shows EC adhesion-% as compared to initial cell density during 26 h culture with 24 h at 37 °C and 2 h at 20 °C incubation. Brush-10−1 showed the highest EC adhesion after 24 h incubation at 37 °C, then EC adhesion decreased in the order: brush-200−0.5 > brush-300−0.5 > brush-300−1 > brush-300−3, respectively, while no EC adhered on brush-300−6. In other words, the smaller the amount of grafted PIPAAm and PIPAAm layer thickness, the larger the number of adhered cells. Adhered ECs on brush-300−0.5, brush-300−1, and brush-300−3 were completely detached after 1 h-incubation at 20 °C, while adhered ECs on TCPS and initiator-modified surfaces were maintained after 2 h incubation at 20 °C. Most of the adhered ECs on brush-200−0.5 and brush-10−1 detached after 2 h incubation at 20 °C under static condition. This indicates that cell adhesion/detachment behavior on PIPAAm brush surfaces was controlled only by temperature, analogous to that on EB-polymerized PIPAAm surfaces [1,3]. In addition, PIPAAm brush layer thickness influenced cell adhesion and detachment behavior. Interestingly, the grafted amount and interfacial layer thickness for PIPAAm brush-300−0.5 were larger than the cross-linked PIPAAm grafted cell culture dishes prepared by EB polymerization method (polymer grafted amount of 2 $\mu g/cm^2$ and ca. 20 nm thickness [18]). Furthermore, brush-10−1 having only 0.4 $\mu g/cm^2$ of PIPAAm chains showed cell detachment during incubation at 20 °C. For EB-grafted PIPAAm surfaces containing less than 1.5 $\mu g/cm^2$ no cell detachment was seen during incubation at 20 °C, although detailed mechanism is unknown at this stage. On the other hand, Xu et al. [33] insisted that the larger the PIPAAm layer thickness (3−31 nm with ATRP reaction time), the higher the amount of adhered 3T3 fibroblasts. However, these data are opposite to the present research: i.e., ECs adhesion decreased with increasing grafted polymer layer thickness and decreasing contact angle of the surfaces. As for the result by Xu et al. [33] the relation between the cell adhesion and surface hydrophobicity is unclear. Difference in the results of the present research and Xu et al. [33] might be arising from the difference in the substrate (silicon substrate and PSt).

We then analyzed FN adsorption at 37 °C on brush-300−0.5 as EC-adhesive surfaces and brush-300−6 as EC-nonadhesive surfaces. FN is one of the most intensively studied components of the ECM proteins, particularly in terms of its effects on

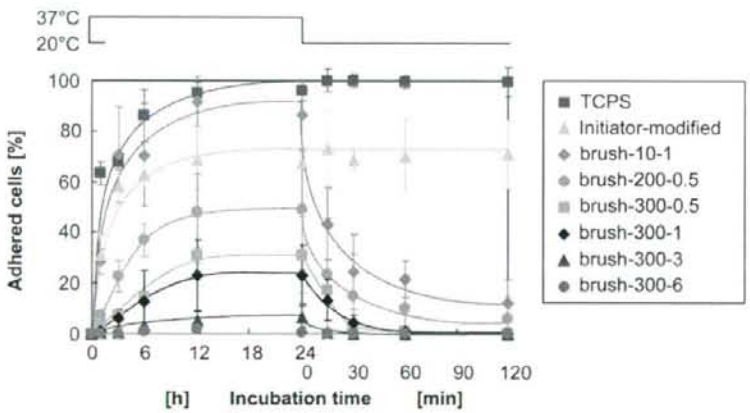

Fig. 5. EC adhesion on and detachment from PIPAAm brush surfaces in cell culture in serum medium. TCPS and ATRP initiator-modified surfaces are used as control surfaces. Symbols: brown square, TCPS; light blue triangle, ATRP initiator-modified surfaces; red diamond, brush-10−1; pink circle, brush-200−0.5; orange square, brush-300−0.5; black diamond, brush-300−1; thick blue triangle, brush-300−3; and green circle, brush-300−6. Data from four separate experiments are shown as mean ± SD.

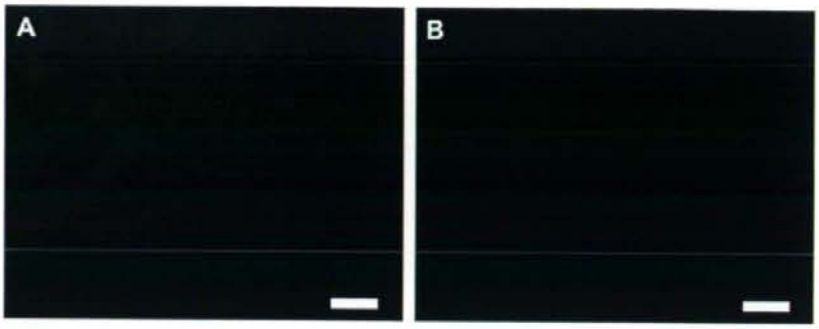

Fig. 6. Fluorescent microscopic images Rhodamine-labelled fibronectin adsorbed to polymer surfaces for (A) brush-300–0.5 and (B) brush-300–6. Scale bars, 100 μm.

cell adhesion. FN plays a central role in ECM adsorption to substrates [37]. Rhodamine-labelled FN was used to visualize FN adsorption on PIPAAm surfaces having different grafted polymer amounts. Reddish fluorescent emission of Rhodamine at 580 nm was imaged with an excitation at 520 nm (Fig. 6). Brush-300–0.5 surfaces were stained with reddish fluorescence arising from Rhodamine-labelled FN while no fluorescence was seen on brush-300–6 at 37 °C, indicating that differences in cell adhesion on brush-300–0.5 and brush-300–6 are due to protein adsorption. Protein adsorption on hydrophilic polymer brushes is controlled by chain length of grafted polymers. Our results agreed with previous reports [38].

Fig. 7 shows a schematic illustration to explain different cell adhesion behavior on brush-300–0.5 and brush-300–6 surfaces. PIPAAm brush surfaces are reported to show different hydration dynamics and phase transition behavior at their outermost surface versus the inner regions of the grafted PIPAAm chains [31,39]. Balamurugan et al. [31] investigated thermoresponsive hydration transition of PIPAAm brush surfaces on gold using surface plasmon resonance (SPR) spectroscopy and contact angle measurements. SPR results showed that PIPAAm brush surfaces undergo a quite broad transition with no sharp changes over a range of 10–40 °C, although contact angle measurements showed a sharp surface property change at 32 °C [31]. Contact angle measurement was reported to be sensitive to the outermost region (0.5–1 nm) of grafted PIPAAm [39]. These results suggest that PIPAAm brush surfaces show different hydration dynamics at their outermost and inner region. Furthermore, Shan et al. [32] proposed the following ideas by the high-sensitivity microcalorimetric measurement of PIPAAm brush surface on gold nanoparticles. The inner regions of the grafted PIPAAm are closely packed, sterically hindered and less hydrated, while the outermost regions of the grafted PIPAAm are more loosely packed and hydrated chain conformation [39]. On the other hand, for PIPAAm brushes on PSt surfaces, brush-300–6 has longer PIPAAm chains than brush-300–0.5. Thus brush-300–6 could plausibly become more hydrated in its outer regions than brush-300–0.5. In addition, more FN molecules adsorbed onto brush-300–0.5 than on brush-300–6. As a result, cell adhesion to brush-300–6 is suppressed. These results suggest that cell adhesion is indirectly controlled by PIPAAm layer thickness.

We also examined whether confluent cell culture is possible on either brush-200–0.5 or brush-300–0.5. Brush-200–0.5

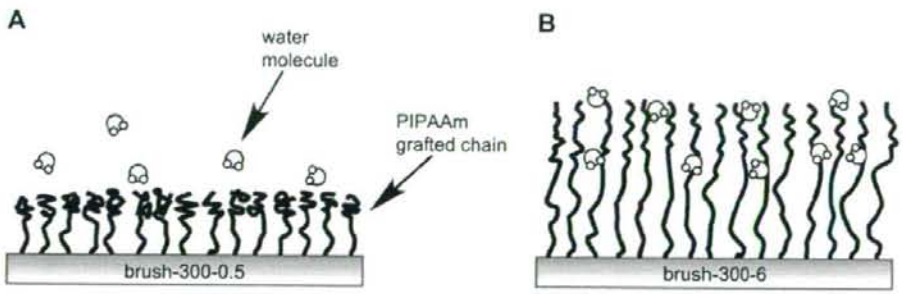

Fig. 7. Schematic illustration of (A) brush-300–0.5 and (B) brush-300–6 based on chain mobility for grafted PIPAAm in aqueous solution at 37 °C. Molecular motion of the grafted PIPAAm chains becomes larger with increasing chain lengths. The inner regions of the grafted PIPAAm are less hydrated and closely packed. As PIPAAm chains exist at distant area from the surface, chain mobility increases. The outer regions of brush-300–0.5 were relatively hydrophobic than brush-300–6 so that FN adsorption and EC adhesion occurred on brush-300–0.5. Brush-300–6 showed suppressed both FN adsorption and EC adhesion.

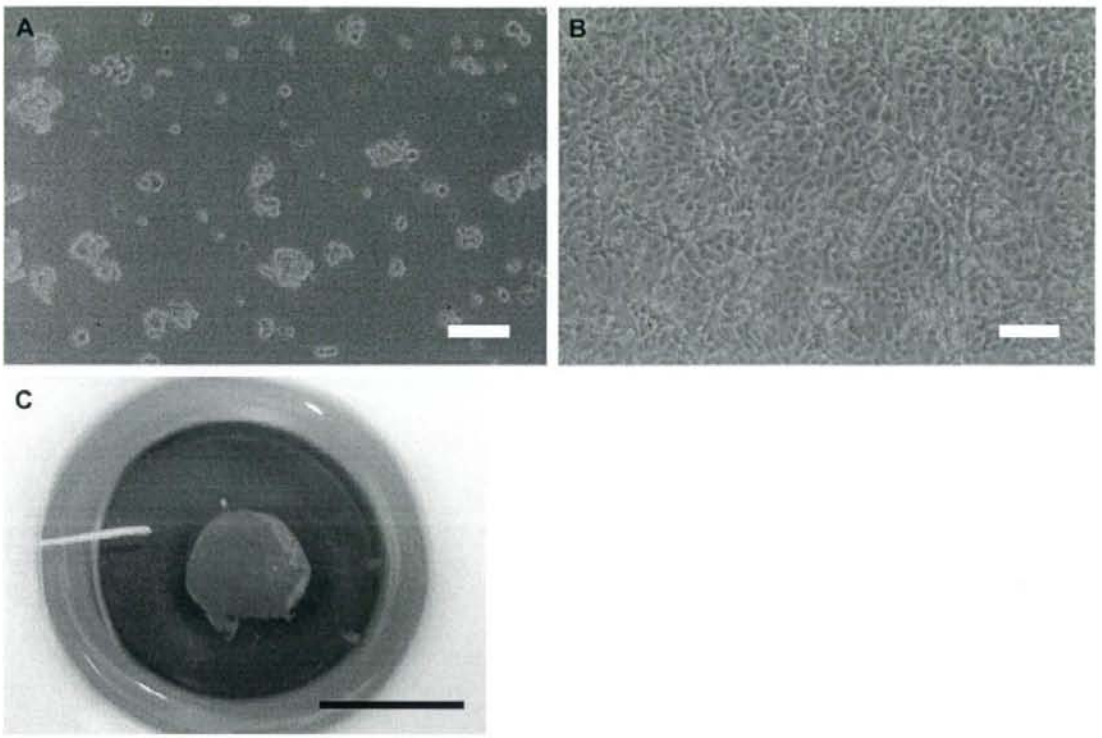

Fig. 8. Morphologies of (A) adhered ECs on brush-300–0.5 after 3 days incubation at 37 °C observed under phase-contrast microscope, (B) confluent cultures of ECs on brush-200–0.5 after 3 days incubation at 37 °C observed under phase-contrast microscope, and (C) detached EC sheet from brush-200–0.5 after 2 h incubation at 20 °C. Scale bars: (A, B) 100 μm and (C) 1 cm.

was selected because this surface contained almost the same PIPAAm grafted amount but with lesser thickness than EB-polymerized PIPAAm surfaces shown in many previous studies to effectively produce confluent cell sheets that detach with temperature reduction [9,10]. However, as can be seen in Fig. 5, brush-200–0.5 surfaces showed ECs adhesion at 37 °C, and almost all of adhered ECs detach at 20 °C incubation. After 3 days incubation at 37 °C with initial cell density of 1.0×10^5 cells/cm^2, ECs on brush-300–0.5 did not proliferate (Fig. 8A). By contrast, ECs on brush-200–0.5 proliferated to reach confluency (Fig. 8B). Thus, we then tried to recover ECs as a cell sheet from brush-200–0.5 by reducing culture temperature. These cells detached completely as an EC monolayer sheet from hydrophilic PIPAAm surfaces produced by 1 h incubation at 20 °C (Fig. 8C). The size of the recovered cell sheet was smaller than the original area of cell culture due to the contractile forces inherent within the cells and their connectivity in the sheet. To prevent shrinkage of the harvested cell sheet, a support membrane has proven useful to manipulate the cell sheet [9,10]. Cell sheets spontaneously physically attach to the support membrane and are harvested with most of adhesive proteins. Therefore, cell sheets are easily transplanted from *in vitro* to *in vivo* [9–13].

4. Conclusions

We prepared thermoresponsive PIPAAm brushes on poly(4-vinylbenzyl chloride)-coated polystyrene surfaces using surface-initiated atom transfer radical polymerization. Successful polymerization was confirmed by surface characterization. We achieved EC adhesion/detachment control using PIPAAm brush surfaces through grafted PIPAAm amounts and their layer thickness. Thicker PIPAAm layers with high polymer grafted amounts showed negligible FN adsorption as well as negligible cell adhesion. Furthermore, we succeeded in preparation of endothelial cell sheets using PIPAAm brush surfaces. Using PIPAAm brush surfaces of an appropriate PIPAAm layer thickness, cells are unable to detach from EB-grafted PIPAAm surfaces. PIPAAm brush interfaces should be useful as a new alternative to EB-grafted surfaces for producing cell sheets to apply in aspects of biotechnology and regenerative medicine.

Acknowledgments

Present research was supported in part by Grant-in-Aid for Scientific Research (Grant No. 1620036) from the Japan Society for Promotion of Science (JSPS), and by a Grant-in-Aid

for the Center of Excellence (COE) program for the 21st Century, "The Center for Tissue Engineering and Regenerative Medicine", from the Ministry of Education, Culture, Sports, Science and Technology (MEXT), Japan. The authors are grateful to Drs. J. Kobayashi and Y. Akiyama, Tokyo Women's Medical University for their technical comments, and to Professor D.W. Grainger, University of Utah for his technical comments as well as English editing.

References

[1] Yamada N, Okano T, Sakai H, Karikusa F, Sawasaki Y, Sakurai Y. Thermo-responsive polymeric surfaces; control of attachment and detachment of cultured cells. Makromol Chem Rapid Commun 1990;11:571–6.

[2] Okano T, Yamada N, Sakai H, Sakurai Y. A novel recovery system for cultured cells using plasma-treated polystyrene dishes grafted with poly(*N*-isopropylacrylamide). J Biomed Mater Res 1993;27:1243–51.

[3] Kikuchi A, Okano T. Nanostructure designs of biomedical materials: applications of cell sheet engineering to functional regenerative tissues and organs. J Control Release 2005;101:69–84.

[4] Kanazawa H, Yamamoto K, Matsushima Y, Takai N, Kikuchi A, Sakurai Y, et al. Temperature-responsive chromatography using poly(*N*-isopropylacrylamide)-modified silica. Anal Chem 1996;68(1):100–5.

[5] Kikuchi A, Okano T. Intelligent thermoresponsive polymeric stationary phases for aqueous chromatography of biological compounds. Prog Polym Sci 2002;27:1165–93.

[6] Heskins M, Guillet JE, James E. Solution properties of poly(*N*-isopropylacrylamide). J Macromol Sci Chem A 1968;2:1441–5.

[7] Bae YH, Okano T, Kim SW. Temperature dependence of swelling of crosslinked poly(*N*,*N*-alkyl substituted acrylamide) in water. J Polym Sci Part B, Polym Phys 1990;28:923–36.

[8] Kobayashi J, Kikuchi A, Sakai K, Okano T. Aqueous chromatography utilizing pH-/temperature-responsive polymer stationary phases to separate ionic bioactive compounds. Anal Chem 2001;73(9):2027–33.

[9] Kikuchi A, Okuhara M, Karikusa F, Sakurai Y, Okano T. Two-dimensional manipulation of confluently cultured vascular endothelial cells using temperature-responsive poly(*N*-isopropylacrylamide)-grafted surfaces. J Biomater Sci Polym Ed 1998;9(12):1331–48.

[10] Hirose M, Kwon OH, Yamato M, Kikuchi A, Okano T. Creation of designed shape cell sheets that are noninvasively harvested and moved onto another surface. Biomacromolecules 2000;1(3):377–81.

[11] Nishida K, Yamato M, Hayashida Y, Watanabe K, Maeda N, Watanabe H, et al. Functional bioengineering corneal epithelial sheet grafts from corneal stem cells expanded ex vivo on a temperature-responsive cell culture surface. Transplantation 2004;77(3):379–85.

[12] Nishida K, Yamato M, Hayashida Y, Watanabe K, Yamamoto K, Adachi E, et al. Corneal reconstruction with tissue-engineered cell sheets composed of autologous oral mucosal epithelium. N Engl J Med 2004;351(12):1187–96.

[13] Ohki T, Yamato M, Murakami D, Takagi R, Yang J, Namiki H, et al. Treatment of oesophageal ulcerations using endoscopic transplantation of tissue engineered autologous oral mucosal epithelial cell sheets in a canine model. Gut 2006;55(12):1704–10.

[14] Hasegawa M, Yamato M, Kikuchi A, Okano T, Ishikawa I. Human periodontal ligament cell sheets can regenerate periodontal ligament tissue in an athymic rat model. Tissue Eng 2005;11(3–4):469–78.

[15] Okano T, Yamada N, Okuhara M, Sakai H, Sakurai Y. Mechanism of cell detachment from temperature-modulated, hydrophilic–hydrophobic polymer surfaces. Biomaterials 1995;16:297–303.

[16] Yamato M, Okuhara M, Karikusa F, Kikuchi A, Sakurai Y, Okano T. Signal transduction and cytoskeletal reorganization are required for cell detachment from cell culture surfaces grafted with a temperature-responsive polymer. J Biomed Mater Res 1999;44:44–52.

[17] Yamato M, Konno C, Kushida A, Hirose M, Utsumi M, Kikuchi A, et al. Release of adsorbed fibronectin from temperature-responsive culture surfaces requires cellular activity. Biomaterials 2000;21:981–6.

[18] Akiyama Y, Kikuchi A, Yamato M, Okano T. Ultrathin poly(*N*-isopropylacrylamide) grafted layer on polystyrene surfaces for cell adhesion/detachment control. Langmuir 2004;20:5506–11.

[19] Canavan HE, Cheng X, Graham DJ, Ratner BD, Castner DG. Surface characterization of the extracellular matrix remaining after cell detachment from a thermoresponsive polymer. Langmuir 2005;21:1949–55.

[20] Canavan HE, Cheng X, Graham DJ, Ratner BD, Castner DG. Cell sheet detachment affects the extracellular matrix: a surface science study comparing thermal liftoff, enzymatic, mechanical methods. J Biomed Mater Res 2005;75A:1–13.

[21] Haraguchi Y, Shimizu T, Yamato M, Kikuchi A, Okano T. Electrical coupling of cardiomyocyte sheets occurs rapidly via functional gap junction formation. Biomaterials 2006;27(27):4765–74.

[22] Stile RA, Healy KE. Thermo-responsive peptide-modified hydrogels for tissue regeneration. Biomacromolecules 2001;2:185–94.

[23] Takezawa T, Yamazaki M, Mori Y, Yonaha T, Yoshizato K. Morphological and immuno-cytochemical characterization of a heterospheroid composed of fibroblasts and hepatocytes. J Cell Sci 1992;101:495–501.

[24] Yamazaki M, Tsuchida M, Kobayashi K, Takezawa T, Mori Y. A novel method to prepare multicellular spheroids from varied cell types. Biotechnol Bioeng 1995;48:17–24.

[25] Matyjaszewski K, Xia J. Atom transfer radical polymerization. Chem Rev 2001;101(9):2921–90.

[26] Wu T, Efimenko K, Genzer J. Combinatorial study of the mushroom-to-brush crossover in surface anchored polyacrylamide. J Am Chem Soc 2002;124:9394–5.

[27] Xiao D, Wirth MJ. Kinetics of surface-initiated atom transfer radical polymerization of acrylamide on silica. Macromolecules 2002;35(8):2919–25.

[28] Xiao D, Zhang H, Wirth M. Chemical modification of the surface of poly(dimethylsiloxane) by atom-transfer radical polymerization of acrylamide. Langmuir 2002;18:9971–6.

[29] Idota N, Kikuchi A, Kobayashi J, Akiyama Y, Sakai K, Okano T. Thermal modulated interaction of aqueous steroids using polymer-grafted capillaries. Langmuir 2006;22:425–30.

[30] Nagase K, Kobayashi J, Kikuchi A, Akiyama Y, Kanazawa H, Okano T. Interfacial property modulation of thermoresponsive polymer brush surfaces and their interaction with biomolecules. Langmuir 2007;23:9409–15.

[31] Balamurugan S, Mendez S, Balamurugan SS, O'Brien II MJ, López GP. Thermal response of poly(*N*-isopropylacrylamide) brushes probed by surface plasmon resonance. Langmuir 2003;19(7):2545–9.

[32] Shan J, Chen J, Nuopponen M, Tenhu H. Two phase transitions of poly(*N*-isopropylacrylamide) brushes bound to gold nanoparticles. Langmuir 2004;20:4671–6.

[33] Xu FJ, Zhong SP, Yung LYL, Kang ET, Neoh KG. Surface-active stimuli-responsive polymer-Si(100) hybrids from surface-initiated atom transfer radical polymerization for control of cell adhesion. Biomacromolecules 2004;5:2392–403.

[34] Ciamrolini M, Nardi N. Five-coordinated high-spin complexes of bivalent cobalt, nickel, copper with tris(2-dimethylaminoethyl)amine. Inorg Chem 1966;5(1):41–4.

[35] Huang X, Wirth MJ. Surface-initiated radical polymerization on porous silica. Anal Chem 1997;69:4577–80.

[36] Brandrup J, Immergut EH, Grulke EA, Abe A, Bloch DR. Polymer handbook. 4th ed. New York: John Wiley and Sons, Inc; 1999.

[37] García AJ, Vega MD, Boettiger D. Modulation of cell proliferation and differentiation through substrate-dependent changes in fibronectin conformation. Mol Biol Cell 1999;10:785–98.

[38] Ma H, Li D, Sheng X, Zhao B, Chilkoti A. Protein-resistant polymer coatings on silicon oxide by surface-initiated atom transfer radical polymerization. Langmuir 2006;22(8):3751–6.

[39] Bain CD, Whitesides GM. Depth sensitivity of wetting: monolayers of omega-mercapto ethers on gold. J Am Chem Soc 1988;110:5897–8.

Subcutaneous transplantation of autologous oral mucosal epithelial cell sheets fabricated on temperature-responsive culture dishes

Haruko Obokata,[1,2] Masayuki Yamato,[2] Joseph Yang,[2] Kohji Nishida,[3] Satoshi Tsuneda,[1] Teruo Okano[2]
[1]*Graduate School of Science and Engineering, Waseda University, 3-4-1 Ohkubo, Shinjuku-ku, Tokyo 169-8555, Japan*
[2]*Institute of Advanced Biomedical Engineering and Science, Tokyo Women's Medical University, 8-1 Kawada-cho, Shinjuku-ku, Tokyo 162-8666, Japan*
[3]*Department of Ophthalmology and Visual Science, Tohoku University Graduate School of Medicine, 1-1 Seiryo-machi, Aoba-ku, Sendai, Miyagi 980-8574, Japan*

Received 2 May 2007; accepted 10 May 2007
Published online 13 December 2007 in Wiley InterScience (www.interscience.wiley.com). DOI: 10.1002/jbm.a.31659

Abstract: The oral mucosa is an attractive cell source for autologous transplantation in human patients who require regenerative therapies of various epithelia. However, the time-course of cellular changes in transplanted oral mucosal epithelia at ectopic sites remains poorly understood. By applying a rat model, we analyzed phenotypic changes in oral mucosal epithelial cell sheets after harvest from temperature-responsive culture dishes and subsequent autologous subcutaneous transplantation. We used monoclonal antibodies to identify epithelial-specific cytokeratins 4, 10, 13, and 14, the stem/progenitor cell marker p63, and proliferating cell nuclear antigen, within the regenerated tissues. Transplanted oral mucosal epithelial cell sheets proliferated during the first week after grafting in conjunction with host inflammation, but then began to degenerate afterward with complete disappearance after 3 weeks. Our findings suggest that host subcutaneous tissues support proliferation and differentiation of the oral mucosal epithelial cell sheets, but are unable to promote maintenance of stem and progenitor cells and therefore cannot produce long-term survivability. © 2007 Wiley Periodicals, Inc. J Biomed Mater Res 86A: 1088–1096, 2008

Key words: cell sheet; tissue engineering autologous cell; phenotypic modulation; progenitor cell

INTRODUCTION

The *ex vivo* expansion of epithelial stem and progenitor cells has become a powerful therapeutic modality to treat a variety of diseases or disorders such as massive burns,[1–3] congenital nevi,[4] epidermolysis bullosa,[5] and corneal surface dysfunction.[6–9] We have previously succeeded in clinical ocular surface reconstruction using autologous oral mucosal epithelial cell sheets fabricated on temperature-responsive culture surfaces.[9] Follow-up of greater than 3 years has revealed that ectopic transplantation of oral epithelial cells can regenerate transparent epithelium on the corneal stroma, and maintain recovered visual acuity. More recently, we also reported endoscopic transplantation of oral mucosal epithelial cell sheets for the prevention of inflammation and constriction of the esophagus after endoscopic submucosal dissection.[10] Oral mucosal epithelial cells have strong proliferative potential, and are available from relatively noninvasive biopsies, making the oral mucosal epithelium an attractive cell source for autologous therapies. In addition, we have previously reported the phenotypic change of oral epithelial cells after transplantation onto the corneal stroma in a rabbit model indicating that oral mucosal epithelial cell sheets may be able to actively respond to mesenchymal signaling to differentiate into specific lineages.[11] However, the fate of autologous oral mucosal epithelial cell sheets after ectopic transplantation remains poorly understood and the nature of stem/progenitor cells that are present within the engineered tissues remains a key factor in the long-term success of ectopic transplantation.

Here, we examined the fate of autologous oral mucosal epithelial cell sheets after ectopic transplantation to the subcutaneous space in a rat model.

Correspondence to: T. Okano; e-mail: tokano@abmes.twmu.ac.jp
Contract grant sponsor: Ministry of Education, Culture, Sports, Science, and Technology in Japan

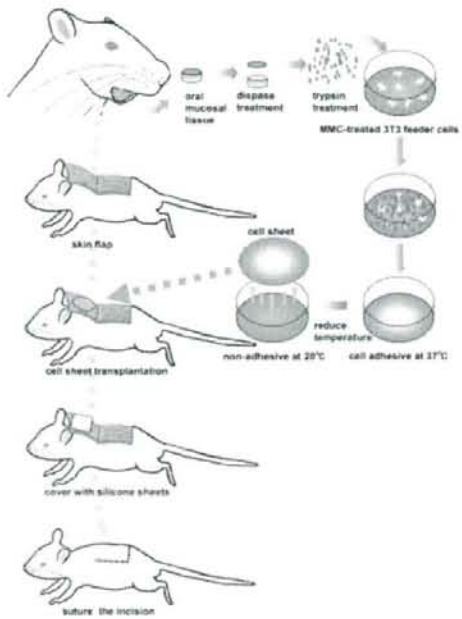

Figure 1. Subcutaneous transplantation of autologous oral mucosal epithelial cell sheets. Autologous oral mucosal epithelial cells are collected and seeded on temperature-responsive culture surfaces. After coculture with a mitomycin C (MMC)-treated 3T3 feeder layer for 8 days, all the cells were harvested as a cell sheet using poly(vinylidene difluoride) (PVDF) membrane after release by temperature reduction. The cell sheet was grafted onto the connective tissue of dorsal skin without sutures and covered with two silicone sheets. Finally, the wounds were closed by sutures. [Color figure can be viewed in the online issue, which is available at www.interscience.wiley.com.]

With this method, engineered tissues are transplanted in an orientation where basal cells attach to connective tissue of dorsal skin and the apical surface of superficial cells is covered by thin silicone sheets to prevent adhesion to the muscle tissues (Fig. 1). This method was first reported in a xenogeneic model with human epidermal cell grafts transplanted into athymic rats and mice as hosts.[12] To exclude the complex results caused by immunorejection, we applied autologous transplantation of oral mucosal epithelial cell sheets to determine the fate of ectopically transplanted tissues.

MATERIALS AND METHODS

Temperature-responsive culture surfaces

The preparation of temperature-responsive culture dishes (CellSeed, Tokyo, Japan) has been previously described.[13] Briefly, *N*-isopropylacrylamide monomer in 2-propanol solution was spread onto 35-mm diameter culture dishes (BD Biosciences, Franklin Lakes, NJ). Dishes were then irradiated by electron beam, resulting in both polymerization and covalent grafting of poly(*N*-isopropylacrylamide) (PIPAAm) onto the cell culture surfaces. PIPAAm-grafted dishes were rinsed with cold-distilled water to remove ungrafted monomer and dried in nitrogen gas. Dishes were finally sterilized with ethylene oxide gas prior to experimental use.

Fabrication of autologous oral mucosal epithelial cell sheets

Animals were treated in accordance with experimental procedures approved by the Committee for Animal Research of Tokyo Women's Medical University. Under deep anesthesia with inhaled isofluorane, oral mucosal biopsies (4 mm in diameter) were obtained from the buccal cavity of Lewis rats (6-week-old, male). Specimens were washed three times with Dulbecco's phosphate-buffered saline (PBS) containing antibiotics and antimycotics, and then incubated at 37°C for 1 h in DMEM containing 1000 units/mL dispase I (Godo Shusei, Tokyo, Japan). Epithelial layers were carefully removed with surgical forceps and treated with 0.25% trypsin-2.65 m*M* EDTA solution (Gibco BRL LifeTechnologies, Grand Island, NY) for 15 min at 37°C to create single-cell suspensions. To prepare lethally treated feeder layers, subconfluent NIH/3T3 cells were incubated with 10 μg/mL mitomycin C for 2 h at 37°C and then trypsinized and seeded onto temperature-responsive culture dishes at a density of 2×10^4 cells/cm^2. The suspended oral mucosal epithelial cells were seeded at a density of 5×10^4 cells/cm^2 onto temperature-responsive culture dishes in the presence of the 3T3 feeder-layers. Epithelial cells were cultured at 37°C in a humidified atmosphere with 5% CO_2 according to the method of Rheinwald and Green.[14]

Autologous transplantation of tissue-engineered oral mucosal epithelial sheets

After culture for 8 days at 37°C, oral mucosal epithelial cells were transferred to another incubator set at 20°C for 30 min. Cell sheets were then noninvasively harvested with the use of a poly(vinylidene difluoride) (PVDF) (Immobilon-P, DURAPORE®, Millipore Corporation, Bedford, MA) support membrane. A 4 cm × 4 cm incision was made in the dorsal skin of each animal with scissors. Harvested autologous epithelial cell sheets were washed with PBS and transplanted onto the skin flap. After 5 min, the support membranes were removed and the transplanted cell sheets were covered with two silicone sheets to avoid adhesion with the underlying muscle tissue and to mimic the environment of original epithelial layer. After transplantation, the incisions were closed with 5-0 nylon sutures (Fig. 1). To observe the time-course of transplanted oral mucosal cell sheets, skin flaps were opened at 1, 3, 5, 7, 10, and 14 days after transplantation ($n = 6$ for each group).